

Electronic Supplementary Information

Boron–nitrogen main chain analogues of polystyrene: poly(*B*-aryl)aminoboranes *via* catalytic dehydrocoupling

*Diego A. Resendiz-Lara, Naomi E. Stubbs, Marius I. Arz, Natalie E. Pridmore,
Hazel A. Sparkes, and Ian Manners**

School of Chemistry, University of Bristol, Cantock's Close, Bristol, BS8 1TS, UK

Content

1) General procedures and equipment	S3
2) Synthesis and characterisation of $\text{NH}_3 \cdot \text{BH}_2\text{Ph}$ (1a) and $\text{NH}_3 \cdot \text{BH}_2(p\text{-CF}_3\text{C}_6\text{H}_4)$ (1b)	S4
3) Thermal studies of $\text{NH}_3 \cdot \text{BH}_2\text{Ph}$ (1a) and $\text{NH}_3 \cdot \text{BH}_2(p\text{-CF}_3\text{C}_6\text{H}_4)$ (1b)	S8
3.1 Thermal studies in the solid state	S8
3.2 Thermal studies in solution	S10
4) Single crystal X-ray diffraction analysis of $[\text{HN-BPh}]_3$ and $[\text{HN-B}(p\text{-CF}_3\text{C}_6\text{H}_4)]_3$	S13
5) Dehydropolymerisation studies of $\text{NH}_3 \cdot \text{BH}_2\text{Ph}$ (1a)	S16
5.1 Dehydropolymerisation of 1a using different catalysts ($[\{\text{Rh}(\text{COD})(\mu\text{-Cl})\}_2]$, $[\text{IrH}_2(\text{POCOP})]$ and skeletal nickel)	S16
5.2 Dehydropolymerisation of 1a with various catalyst loadings of $[\text{IrH}_2(\text{POCOP})]$	S18
5.3 Dehydropolymerisation of 1a with 1 mol % $[\text{IrH}_2(\text{POCOP})]$ after various reaction times	S21
6) Synthesis and Characterisation of poly(<i>B</i> -aryl aminoboranes)	S24
6.1 Synthesis and characterisation of $[\text{NH}_2\text{-BPh}]_n$ (2a)	S24
6.2 Synthesis and characterisation $[\text{NH}_2\text{-BH}(p\text{-CF}_3\text{C}_6\text{H}_4)]_n$ (2b)	S27
6.3 GPC analysis of 2a and 2b at different concentrations	S30
6.4 DLS analysis of 2a and 2b	S32
7) Thermal studies of $[\text{NH}_2\text{-BPh}]_n$ (2a) and $[\text{NH}_2\text{-BH}(p\text{-CF}_3\text{C}_6\text{H}_4)]_n$ (2b)	S33
7.1 Thermal studies in the solid State	S33
7.2 Thermal studies in solution	S36
8) References	S42

1) General procedures and equipment

All manipulations were carried out under an atmosphere of nitrogen using standard vacuum line and Schlenk techniques, or under an atmosphere of argon within an MBraun glovebox. All solvents were dried via a Grubbs design solvent purification system.^{S1} Phenyl boronic acid (PhB(OH)₂), *p*-trifluoromethylphenyl boronic acid [(*p*-CF₃C₆H₄)B(OH)₂], lithium aluminium hydride (LiAlH₄), ammonium chloride (NH₄Cl), Celite and chloro(1,5-cyclooctadiene)rhodium(I) dimer ([{Rh(COD)(μ-Cl)}₂]) were purchased from Sigma Aldrich Ltd. and used as acquired. [IrH₂(POCOP)] (POCOP = [κ³-1,3-(*t*Bu₂PO)₂C₆H₃]^{S2} and skeletal nickel^{S3} were synthesised via literature methods and purified by re-precipitation ([IrH₂(POCOP)]) and washing with *n*-hexane (skeletal nickel). The NMR spectra were recorded at 298 K in J. Young quartz-glass NMR on Jeol ECP(Eclipse) 300 or Jeol ECP(Eclipse) 400 spectrometers. Anhydrous chloroform-*d* and THF-*d*₈ were purchased from Sigma Aldrich Ltd. and stored over molecular sieves (4 Å) in the glovebox. The ¹H and ¹³C NMR spectra were calibrated against the residual ¹H and ¹³C resonances of the respective deuterated solvent [chloroform-*d*: δ(¹H) = 7.24 ppm, δ(¹³C) = 77.0 ppm; dichloromethane-*d*₂: δ(¹H) = 5.32 ppm, δ(¹³C) = 54.0 ppm; THF-*d*₈: δ(¹H) = 1.73 ppm, δ(¹³C) = 25.4 ppm] relative to tetramethylsilane [δ(¹H) = 0.00 ppm, δ(¹³C) = 0.0 ppm]. The ¹¹B NMR spectra were calibrated against external neat BF₃·Et₂O [δ(¹¹B) = 0.0 ppm]. Integration of ¹¹B NMR spectra was performed using MestReNova Version 7.1.1 with an estimated accuracy of ± 5%. ESI mass spectra were recorded on a Bruker Daltonics Apex IV Fourier transform Ion Cyclotron resonance mass spectrometer with a cone potential of +150 V using the negative mode in THF or acetonitrile. Elemental analysis was performed with a Eurovector EA 3000 Elemental Analyser at the University of Bristol Microanalysis Laboratory. Gel permeation chromatography (GPC) was performed on a Malvern RI max Gel Permeation Chromatograph, equipped with an automatic sampler, a pump, an injector, and inline degasser. The columns (T5000) were contained within an oven (35 °C) and consisted of styrene/divinyl benzene gels. Sample elution was detected by means of a differential refractometer. THF (Fisher), containing 0.1 wt% [*n*Bu₄N]Br, was used as the eluent at a flow rate of 1 mL min⁻¹. Samples were dissolved in the eluent (2 mg mL⁻¹) and filtered with a Ministart SRP15 filter [poly(tetrafluoroethylene) membrane of 0.45 μm pore size] before analysis. The calibration was conducted using monodisperse polystyrene standards obtained from Sigma Aldrich. The lowest (highest) molecular weight standard used was 2,300 (994,000) g mol⁻¹. Dynamic light scattering (DLS) experiments were carried out using a Malvern Zetasizer Nano S spectrometer using a He-Ne laser (λ = 632 nm) in a gas-tight glass cuvette in dry CH₂Cl₂. Thermogravimetric analysis (TGA) was performed on a Thermal Advantage TGAQ500 with a heating rate of 10 °C min⁻¹ under nitrogen. The TGA results were analysed using WinUA V4.5A by Thermal Advantage.

2) Synthesis and characterisation of $\text{NH}_3\cdot\text{BH}_2\text{Ph}$ (**1a**) and $\text{NH}_3\cdot\text{BH}_2(p\text{-CF}_3\text{C}_6\text{H}_4)$ (**1b**)

Synthesis of $\text{NH}_3\cdot\text{BH}_2\text{Ph}$ (1a**):** To a suspension of LiAlH_4 (2.29 g, 60.3 mmol) in Et_2O (50 mL) was added a solution of PhB(OH)_2 (5 g, 40.2 mmol) in Et_2O / toluene (50 mL, 5:2) at 20°C and the suspension was stirred at this temperature for 2 h. The mixture was filtered via cannula to yield a solution of $\text{Li[BH}_3\text{Ph]}$. This solution was added to a suspension of NH_4Cl (3.23 g, 60.3 mmol) in Et_2O (50 mL) at -78°C and the mixture was stirred overnight in the cold bath until it reached room temperature. The next day the reaction mixture was filtered through Celite. Removal of the solvent from the clear colourless filtrate and drying of the residue under vacuum at room temperature yielded compound **1a** a colourless oil, which solidifies at low temperature (-40°C). Yield: 1.6 g (15.8 mmol, 39 %).

^{11}B NMR (96 MHz, CDCl_3): $\delta = -13.9$ (t, $^1J_{\text{BH}} = 95$ Hz) (Figure S1).

^1H NMR (400 MHz, CDCl_3): $\delta = 2.36$ (2 H, q, br, $^1J_{\text{BH}} = 95$ Hz, BH_2), 3.12 (3 H, br, NH_3), 7.16 (1 H, t, $^3J_{\text{HH}} = 4$ Hz, *para*-ArH), 7.25-7.31 (4 H, m, *meta*-ArH + *ortho*-ArH) (Figure S3).

$^{13}\text{C}\{^1\text{H}\}$ NMR (101 MHz, CDCl_3): $\delta = 125.8$ (ArC), 127.9 (ArC), 131.9 (ArC), 133.7 (ArC) (Figure S4).

Elemental analysis calcd (%) for $\text{C}_6\text{H}_{10}\text{BN}$: C 67.37, H 9.42, N 13.10; found: C 67.66, H 9.67, N 13.13.

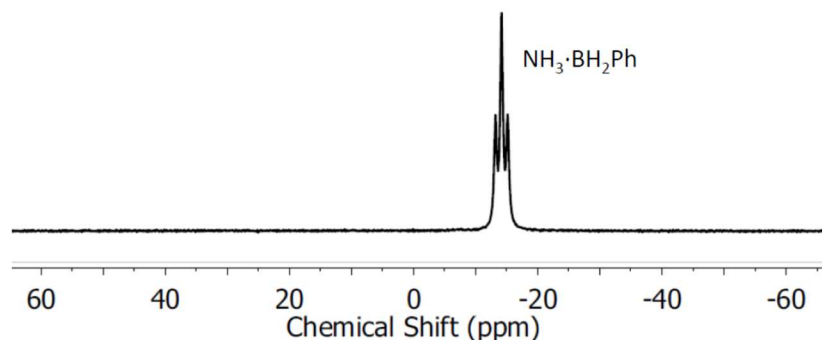


Figure S1. ^{11}B NMR spectrum of $\text{NH}_3\cdot\text{BH}_2\text{Ph}$ (**1a**) in CDCl_3

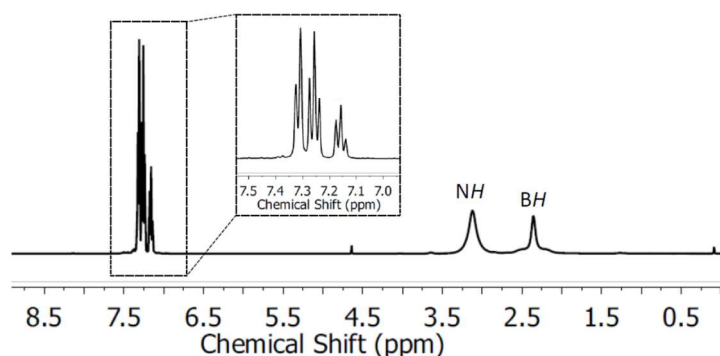


Figure S2. $^1\text{H}\{^{11}\text{B}\}$ NMR spectrum of $\text{NH}_3\cdot\text{BH}_2\text{Ph}$ (**1a**) in CDCl_3 .

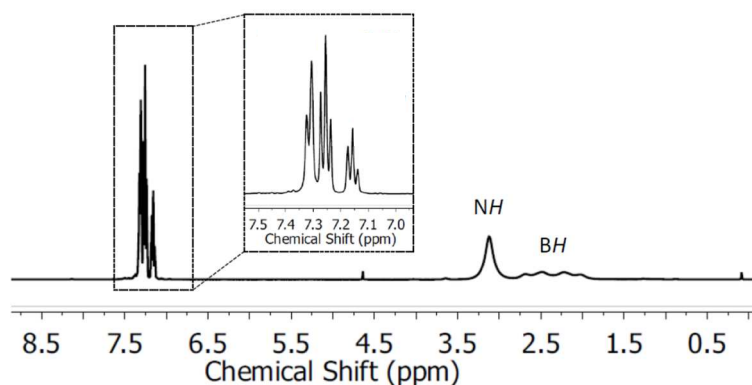


Figure S3. ^1H NMR spectrum of $\text{NH}_3\cdot\text{BH}_2\text{Ph}$ (**1a**) in CDCl_3 .

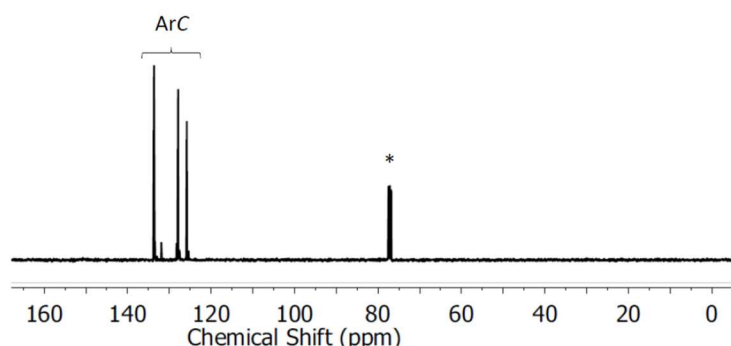


Figure S4. $^{13}\text{C}\{^1\text{H}\}$ NMR spectrum of $\text{NH}_3\cdot\text{BH}_2\text{Ph}$ (**1a**) in CDCl_3 . * CDCl_3 .

Synthesis of $\text{NH}_3\cdot\text{BH}_2(p\text{-CF}_3\text{C}_6\text{H}_4)$ (1b**):** To a suspension of LiAlH_4 (1.47 g, 38.7 mmol) in Et_2O (50 mL) was added a solution of $(p\text{-CF}_3\text{C}_6\text{H}_4)\text{B}(\text{OH})_2$ (5 g, 26.3 mmol) in Et_2O / toluene (50 mL, 5:2) at 20°C and the suspension was stirred at this temperature for 2 h. The mixture was filtered via cannula to yield a solution of $\text{Li}[\text{BH}_3(p\text{-CF}_3\text{C}_6\text{H}_4)]$. This solution was added to a suspension of NH_4Cl (3.23 g, 60.3 mol) in Et_2O (50 mL) at 20°C and the suspension was stirred overnight in the cold bath until it reached room temperature. The next day the reaction mixture was filtered through celite. Removal of the solvent from the clear, colourless filtrate and drying of the residue under vacuum afforded compound **1b** as a colourless solid. Yield: 3.12 g (17.8 mmol, 69 %).

^{11}B NMR (96 MHz, $\text{THF-}d_8$): $\delta = -16.8$ (t, $^1J_{\text{BH}} = 96$ Hz) (Figure S5).

^1H NMR (400 MHz, $\text{THF-}d_8$): $\delta = 2.45$ (2 H, q, br, $^1J_{\text{BH}} = 96$ Hz, BH_2), 4.57 (3 H, br, NH_3), 7.34 (4 H, m, *meta*-ArH + *ortho*-ArH) (Figure S6).

$^{13}\text{C}\{^1\text{H}\}$ NMR (101 MHz, $\text{THF-}d_8$): $\delta = 120.9$ (q, $^3J_{\text{FC}} = 4$ Hz, *meta*-ArC), 123.3 (q, $^1J_{\text{FC}} = 270$ Hz, ArCF_3), 123.8 (q, $^2J_{\text{FC}} = 31$ Hz, *para*-ArC), 131.1 (*ortho*-ArC) (the signal for the B-bonded *ipso*-ArC atom was not detected) (Figure S7).

$^{19}\text{F}\{^1\text{H}\}$ NMR (376 MHz, $\text{THF-}d_8$): $\delta = -64.4$ (s) (Figure S8).

Elemental analysis calcd (%) for $C_7H_9BF_3N$: C 48.05, H 5.19, N 8.01; found: C 48.15, H 5.17, N 7.49.

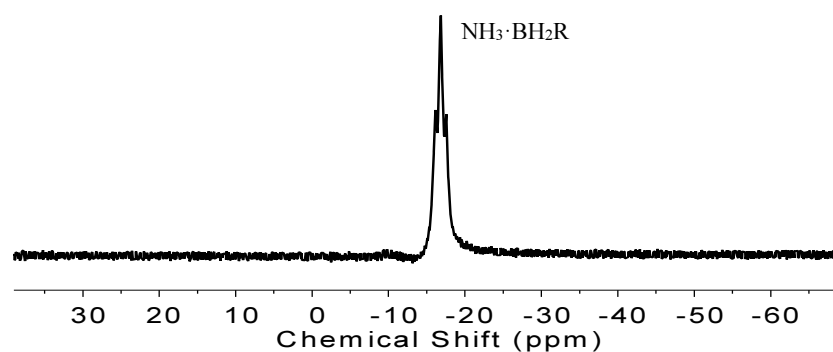


Figure S5. ^{11}B NMR spectrum of $NH_3 \cdot BH_2(p-CF_3C_6H_4)$ (**1b**) in $THF-d_8$. R = $p-CF_3C_6H_4$

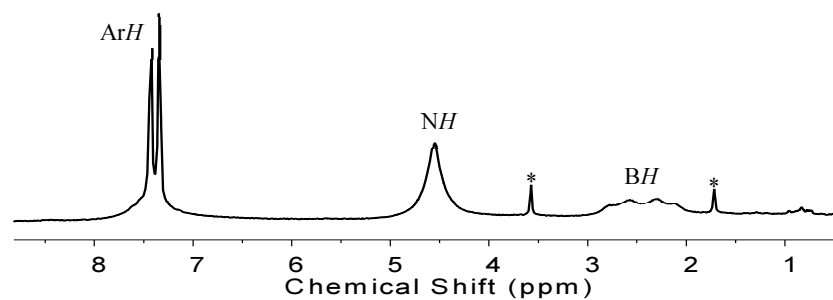


Figure S6. 1H NMR spectrum of $NH_3 \cdot BH_2(p-CF_3C_6H_4)$ (**1b**) in $THF-d_8$. * $THF-d_8$.

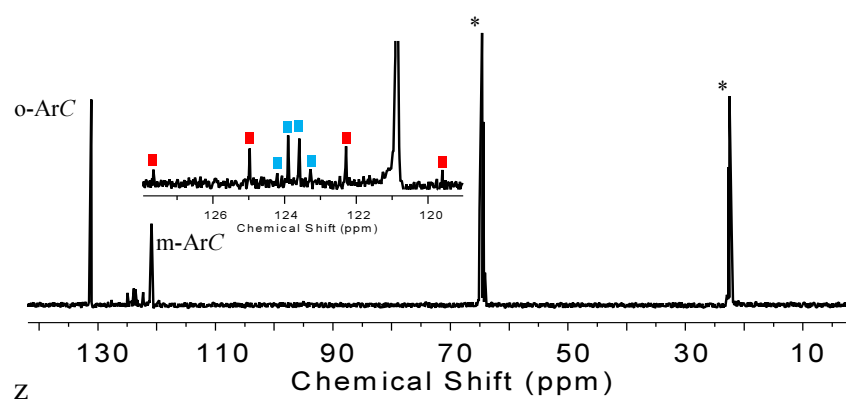


Figure S7. $^{13}C\{^1H\}$ NMR spectrum of $NH_3 \cdot BH_2(p-CF_3C_6H_4)$ (**1b**) in $THF-d_8$. Red squares: $ArCF_3$. Blue squares: $p-ArC$. * $THF-d_8$.

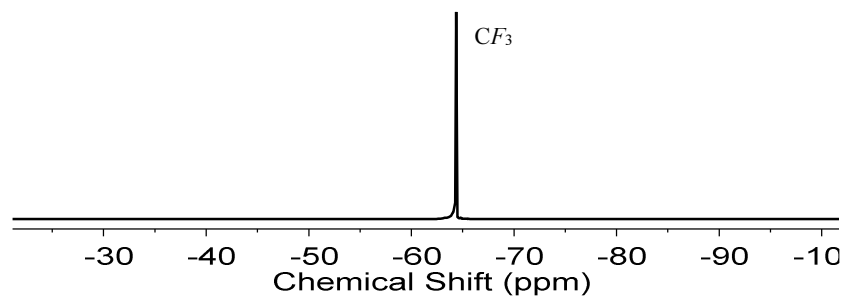


Figure S8. $^{19}\text{F}\{^1\text{H}\}$ NMR spectrum of $\text{NH}_3\cdot\text{BH}_2(p\text{-CF}_3\text{C}_6\text{H}_4)$ (**1b**) in $\text{THF-}d_8$.

3) Thermal studies of $\text{NH}_3\cdot\text{BH}_2\text{Ph}$ (**1a**) and $\text{NH}_3\cdot\text{BH}_2(p\text{-CF}_3\text{C}_6\text{H}_4)$ (**1b**)

3.1 Thermal studies in the solid state:

Thermal stability of solid $\text{NH}_3\cdot\text{BH}_2\text{Ph}$ (1a**) at 20 °C:** Solid $\text{NH}_3\cdot\text{BH}_2\text{Ph}$ (53 mg, 0.5 mmol) was allowed to stand at 20 °C. After 170 h, the solid was dissolved in THF (0.4 mL) and analysed by ^{11}B NMR spectroscopy to reveal partial consumption of $\text{NH}_3\cdot\text{BH}_2\text{Ph}$ [δ_{B} -14.0 (t, $^1J_{\text{BH}} = 83$ Hz)] (*ca.* 75 %) to yield $[\text{NH}_2\text{-BHPH}]_n$ [δ_{B} -7.2 (br)] (*ca.* 20 %) and $\text{NH}_3\cdot\text{BH}_3$ [δ_{B} -22.9 (q, $^1J_{\text{BH}} = 107$ Hz)] (*ca.* 5 %) (Figures S9 and S10).

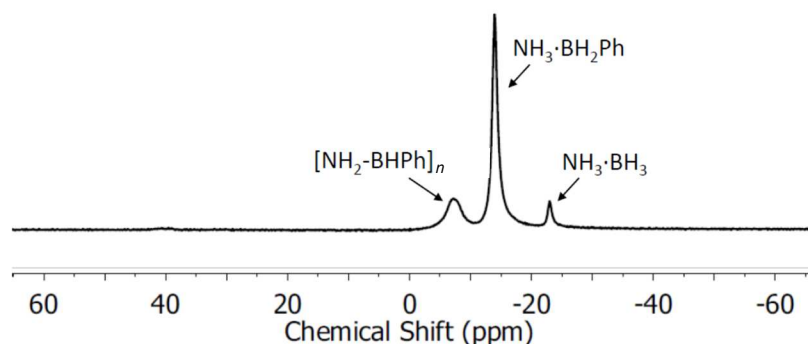


Figure S9. $^{11}\text{B}\{^1\text{H}\}$ NMR spectrum of $\text{NH}_3\cdot\text{BH}_2\text{Ph}$ (**1a**) in THF after leaving as a solid at 20 °C for 170 h.

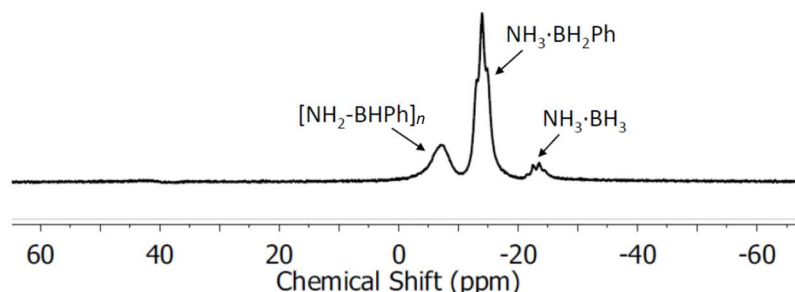


Figure S10. ^{11}B NMR spectrum of $\text{NH}_3\cdot\text{BH}_2\text{Ph}$ (**1a**) in THF after leaving as a solid at 20 °C for 170 h.

Thermal stability of solid $\text{NH}_3\cdot\text{BH}_2\text{Ph}$ (1a**) at 70 °C:** Solid $\text{NH}_3\cdot\text{BH}_2\text{Ph}$ (53 mg, 0.5 mmol) was transferred to a J. Young quartz-glass NMR tube and heated to 70 °C for 170 h. After cooling to 20 °C, the solid was dissolved in THF (0.4 mL) and analysed by ^{11}B NMR spectroscopy indicating quantitative consumption of $\text{NH}_3\cdot\text{BH}_2\text{Ph}$ [δ_{B} -15.3 (t, $^1J_{\text{BH}} = 95$ Hz)] (trace amounts) to yield $\text{H}_2\text{N}=\text{BPh}_2$ [δ_{B} 40.0 (br)] (*ca.* 10 %), $[\text{HN-BPh}]_3$ [δ_{B} 31.4 (s)] (*ca.* 85 %), $\text{NH}_3\cdot\text{BHPH}_2$ [δ_{B} -9.3 (d, $^1J_{\text{BH}} = 87$ Hz)] (*ca.* 5 %) and $\text{NH}_3\cdot\text{BH}_3$ [δ_{B} -23.9 (m)] (trace amounts) (Figures S11 and S12).

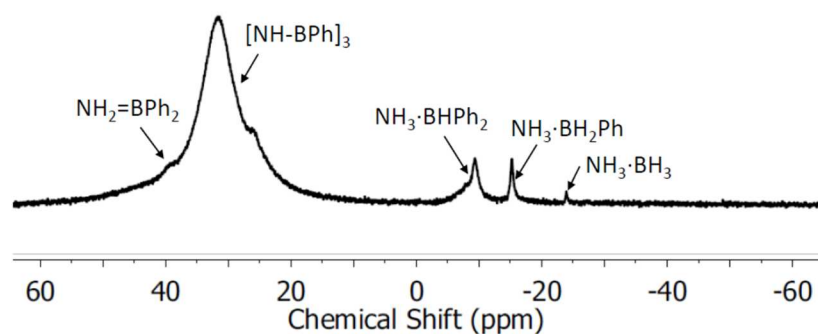


Figure S11. $^{11}\text{B}\{^1\text{H}\}$ NMR spectrum of $\text{NH}_3\cdot\text{BH}_2\text{Ph}$ (**1a**) as in THF after heating as a solid at $70\text{ }^\circ\text{C}$ for 170 h.

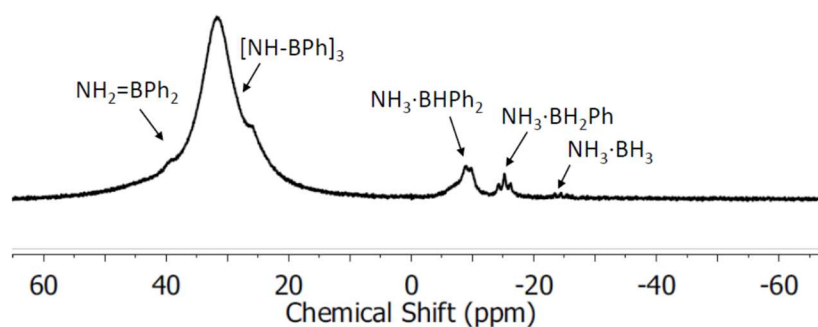


Figure S12. ^{11}B NMR spectrum of $\text{NH}_3\cdot\text{BH}_2\text{Ph}$ (**1a**) in THF after heating as a solid at $70\text{ }^\circ\text{C}$ for 170 h.

Thermal stability of solid $\text{NH}_3\cdot\text{BH}_2(p\text{-CF}_3\text{C}_6\text{H}_4)$ (1b**) at $20\text{ }^\circ\text{C}$:** Solid $\text{NH}_3\cdot\text{BH}_2(p\text{-CF}_3\text{C}_6\text{H}_4)$ (88 mg, 0.5 mmol) was allowed to stand at $20\text{ }^\circ\text{C}$. After 170 h, the solid was dissolved in THF (0.4 mL) and analysed by ^{11}B NMR spectroscopy to reveal no change [$\delta_{\text{B}} -14.8$ (t, $^1J_{\text{BH}} = 96$ Hz)] (Figure S13).

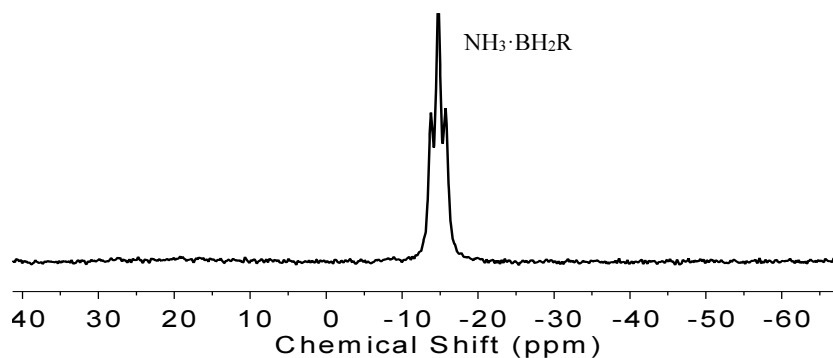


Figure S13. $^{11}\text{B}\{^1\text{H}\}$ NMR spectrum of $\text{NH}_3\cdot\text{BH}_2(p\text{-CF}_3\text{C}_6\text{H}_4)$ (**1a**) in THF after leaving as a solid at $20\text{ }^\circ\text{C}$ for 170 h. R = $p\text{-CF}_3\text{C}_6\text{H}_4$.

Thermal stability of solid $\text{NH}_3 \cdot \text{BH}_2(p\text{-CF}_3\text{C}_6\text{H}_4)$ (1b**) at 70 °C:** Solid $\text{NH}_3 \cdot \text{BH}_2(p\text{-CF}_3\text{C}_6\text{H}_4)$ (88 mg, 0.5 mmol) was transferred to a J. Young quartz-glass NMR tube and heated to 70 °C for 170 h. After cooling to 20 °C, the solid was dissolved in THF (0.4 mL) and analysed by ^{11}B NMR spectroscopy indicating quantitative consumption of $\text{NH}_3 \cdot \text{BH}_2(p\text{-CF}_3\text{C}_6\text{H}_4)$ to yield $[\text{NH}_2\text{-BHR}]_n$ [δ_{B} -6.0], $[\text{HN-B}(p\text{-CF}_3\text{C}_6\text{H}_4)]_3$ [δ_{B} -32.1] and an array of unknown boron-containing species (Figure S14 and S15).

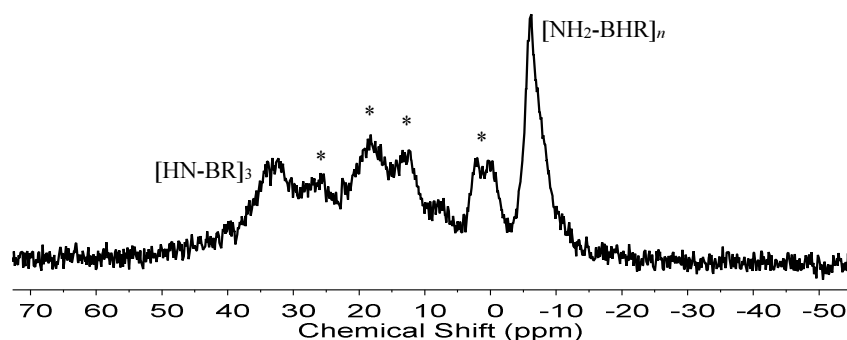


Figure S14. $^{11}\text{B}\{^1\text{H}\}$ NMR spectrum of $\text{NH}_3 \cdot \text{BH}_2(p\text{-CF}_3\text{C}_6\text{H}_4)$ (**1b**) in THF after heating as a solid at 70 °C for 170 h. * Unknown species. R = $p\text{-CF}_3\text{C}_6\text{H}_4$.

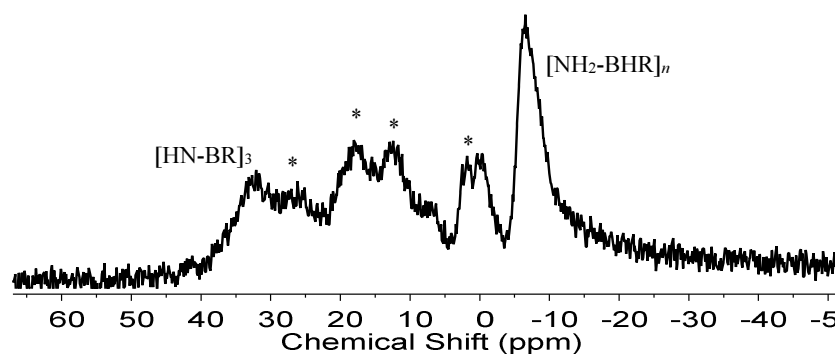


Figure S15. ^{11}B NMR spectrum of $\text{NH}_3 \cdot \text{BH}_2(p\text{-CF}_3\text{C}_6\text{H}_4)$ (**1b**) in THF after heating as a solid at 70 °C for 170 h. * Unknown species. R = $p\text{-CF}_3\text{C}_6\text{H}_4$.

3.2 Thermal studies in solution

Thermal stability of $\text{NH}_3 \cdot \text{BH}_2\text{Ph}$ (1a**) in THF at 20 °C:** A solution of $\text{NH}_3 \cdot \text{BH}_2\text{Ph}$ (53 mg, 0.5 mmol) in THF (2 mL) was stirred for 170 h at 20 °C. The solution was analysed by ^{11}B NMR spectroscopy to reveal no change [δ_{B} -14.2 (t, $^1J_{\text{BH}}$ = 95 Hz)] (Figure S16).

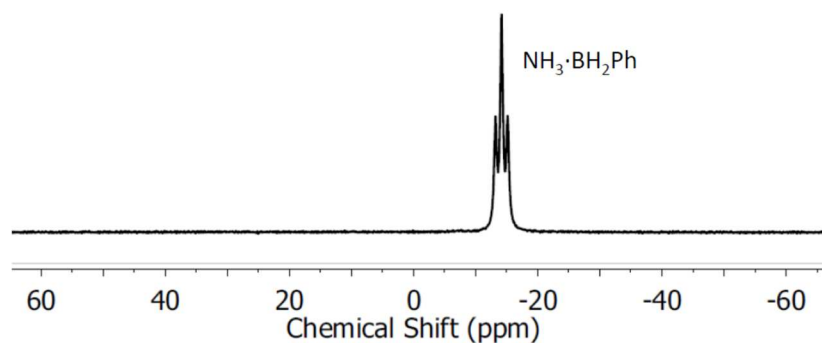


Figure S16. ^{11}B NMR spectrum of $\text{NH}_3\cdot\text{BH}_2\text{Ph}$ (**1a**) in THF at 20 °C after 170 h.

Thermal stability of $\text{NH}_3\cdot\text{BH}_2\text{Ph}$ (1a**) in THF at 70 °C:** An aliquot (0.7 mL) of a solution of $\text{NH}_3\cdot\text{BH}_2\text{Ph}$ (53 mg, 0.5 mmol) in THF (2 mL) was transferred to a J. Young quartz-glass NMR tube and heated to 70 °C for 170 h. After cooling to 20 °C, the mixture was analysed by ^{11}B NMR spectroscopy indicating quantitative consumption of $\text{NH}_3\cdot\text{BH}_2\text{Ph}$ [δ_{B} -14.2 (t, $^1J_{\text{BH}}$ = 91 Hz)] (trace amounts) to yield $\text{H}_2\text{N}=\text{BPh}_2$ [δ_{B} 40.2 (s)] (*ca.* 10 %), $[\text{HN-BPh}]_3$ [δ_{B} 31.6 (s)] (*ca.* 70 %), $[\text{NH}_2\text{-BPh}]_n$ [δ_{B} -6.2 (br)] (*ca.* 10 %), $\text{NH}_3\cdot\text{BPhPh}_2$ [δ_{B} -8.4 (d, $^1J_{\text{BH}}$ = 97 Hz)] (*ca.* 10 %) and an unidentified product [δ_{B} -11.4 (s)] (trace amounts) (Figures S17 and S18).

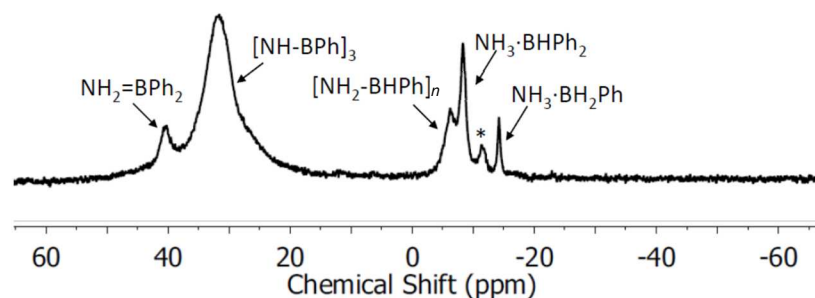


Figure S17. $^{11}\text{B}\{^1\text{H}\}$ NMR spectrum of $\text{NH}_3\cdot\text{BH}_2\text{Ph}$ (**1a**) in THF after heating to 70 °C for 170 h.
* Unassigned product.

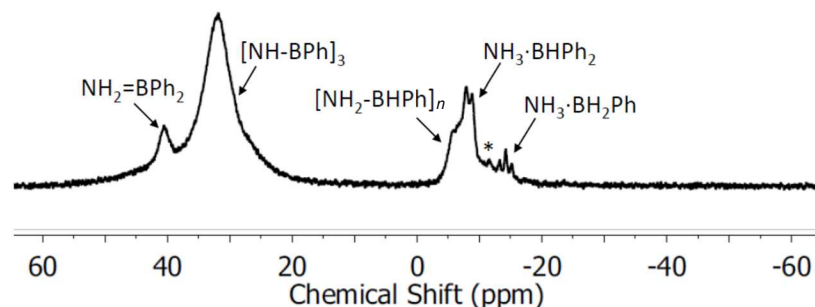


Figure S18. ^{11}B NMR spectrum of $\text{NH}_3\cdot\text{BH}_2\text{Ph}$ (**1a**) in THF after heating to 70 °C for 170 h. * Unassigned product.

Thermal stability of $\text{NH}_3 \cdot \text{BH}_2(p\text{-CF}_3\text{C}_6\text{H}_4)$ (1b**) in THF at 20 °C:** A solution of $\text{NH}_3 \cdot \text{BH}_2(p\text{-CF}_3\text{C}_6\text{H}_4)$ (88 mg, 0.5 mmol) in THF (2 mL) was stirred for 170 h at 20 °C. The solution was analysed by ^{11}B NMR spectroscopy to reveal no change [$\delta_{\text{B}} -14.8$ (t, $^1J_{\text{BH}} = 96$ Hz)] (Figure S19).

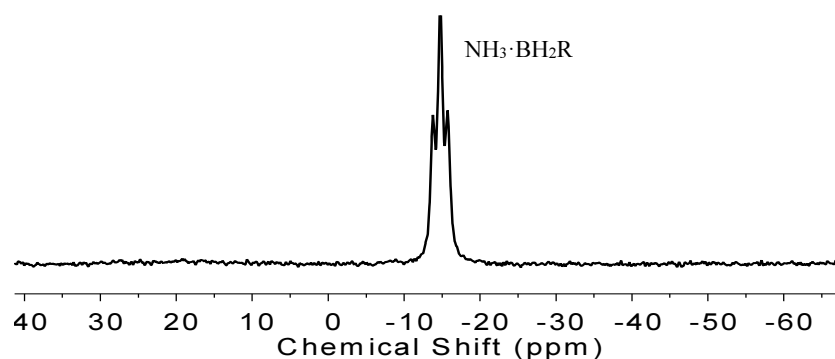


Figure S19. ^{11}B NMR spectrum of $\text{NH}_3 \cdot \text{BH}_2(p\text{-CF}_3\text{C}_6\text{H}_4)$ (**1b**) in THF at 20 °C after 170 h. R = $p\text{-CF}_3\text{C}_6\text{H}_4$.

Thermal stability of $\text{NH}_3 \cdot \text{BH}_2(p\text{-CF}_3\text{C}_6\text{H}_4)$ (1b**) in THF at 70 °C:** An aliquot (0.7 mL) of a solution of $\text{NH}_3 \cdot \text{BH}_2(p\text{-CF}_3\text{C}_6\text{H}_4)$ (88 mg, 0.5 mmol) in THF (2 mL) was transferred to a J. Young quartz-glass NMR tube and heated to 70 °C for 170 h. After cooling to 20 °C, the mixture was analysed by ^{11}B NMR spectroscopy indicating quantitative consumption of $\text{NH}_3 \cdot \text{BH}_2(p\text{-CF}_3\text{C}_6\text{H}_4)$ to yield $[\text{HN-B}(p\text{-CF}_3\text{C}_6\text{H}_4)]_3$ [$\delta_{\text{B}} 31.5$ (s)] (ca. 80 %), $[\text{NH}_2\text{-BH}(p\text{-CF}_3\text{C}_6\text{H}_4)]_n$ [$\delta_{\text{B}} -6.1$ (br)] (ca. 15 %) and an unidentified product [$\delta_{\text{B}} 9.3$ (s, br)] (ca. 5 %) (Figures S20 and S21).

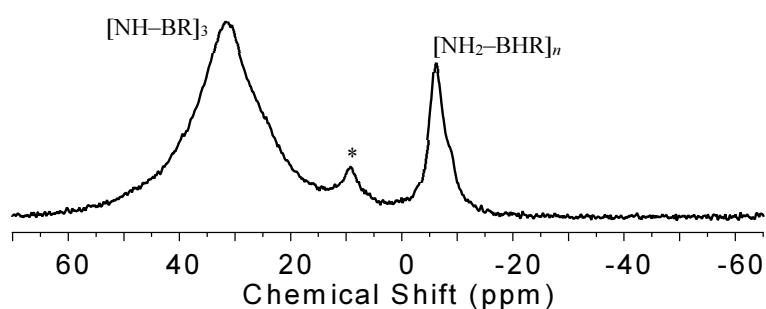


Figure S20. $^{11}\text{B}\{^1\text{H}\}$ NMR spectrum of $\text{NH}_3 \cdot \text{BH}_2(p\text{-CF}_3\text{C}_6\text{H}_4)$ (**1b**) in THF after heating to 70 °C for 170 h. * Unassigned product. R = $p\text{-CF}_3\text{C}_6\text{H}_4$.

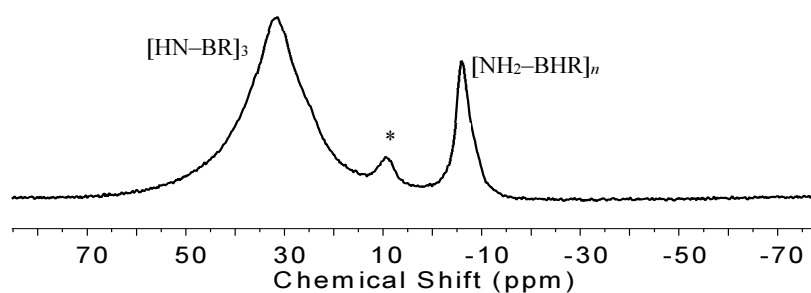


Figure S21. ^{11}B NMR spectrum of $\text{NH}_3 \cdot \text{BH}_2(p\text{-CF}_3\text{C}_6\text{H}_4)$ (**1b**) in THF after heating to 70 °C for 170 h.

* Unassigned product. R = $p\text{-CF}_3\text{C}_6\text{H}_4$.

4) Single crystal X-ray diffraction analysis of $[\text{HN-BPh}]_3$ and $[\text{HN-B}(p\text{-CF}_3\text{C}_6\text{H}_4)]_3$

Single crystals of $[\text{HN-BPh}]_3$ were isolated upon crystallization from a toluene/diethyl ether mixture at -40 °C and single crystals of $[\text{HN-B}(p\text{-CF}_3\text{C}_6\text{H}_4)]_3$ were obtained from a *n*-hexane/diethyl ether mixture at room temperature. X-ray diffraction experiments on $[\text{HN-BPh}]_3$ and $[\text{HN-B}(p\text{-CF}_3\text{C}_6\text{H}_4)]_3$ were carried out at 100(2) K on a Bruker APEX II CCD diffractometer using Mo- K_α radiation ($\lambda = 0.71073$ Å). Intensities were integrated in SAINT^{S4} and absorption corrections based on equivalent reflections using SADABS^{S5} were applied. The structure of $[\text{HN-BPh}]_3$ was solved using Superflip^{S6-S7} and the structure of $[\text{HN-B}(p\text{-CF}_3\text{C}_6\text{H}_4)]_3$ was solved using olex2.solve;^{S8} both structures were refined against F^2 in SHELXL^{S9-S10} using Olex2.^{S11} All non-hydrogen atoms were refined anisotropically. All hydrogen atoms were located geometrically and refined using a riding model, apart from the N-H protons, which were located in the difference map and refined freely. Squeeze within Platon^{S12-S13} was used to remove disordered solvent from the lattice of $[\text{HN-BPh}]_3$ that could not be sensibly modelled. In the case of $[\text{HN-B}(p\text{-CF}_3\text{C}_6\text{H}_4)]_3$ the structure was refined as a two component twin against an hklf5 file with the refined occupancies of the two domains 0.44:0.56. In addition, in $[\text{HN-B}(p\text{-CF}_3\text{C}_6\text{H}_4)]_3$, the CF_3 groups were disordered; the occupancies of the fragments were determined by refining them against a free variable with the sum of the two sites set to equal 1, and the occupancies were then fixed at the refined values. Restraints were applied to maintain sensible geometries and thermal parameters. Crystal structure and refinement data are given in Table 1. Crystallographic data for compounds $[\text{HN-BPh}]_3$ and $[\text{HN-B}(p\text{-CF}_3\text{C}_6\text{H}_4)]_3$ have been deposited with the Cambridge Crystallographic Data Centre as supplementary publication CCDC 1562257-1562258. Copies of the data can be obtained free of charge on application to CCDC, 12 Union Road, Cambridge CB2 1EZ, UK [fax(+44) 1223 336033, e-mail: deposit@ccdc.cam.ac.uk].

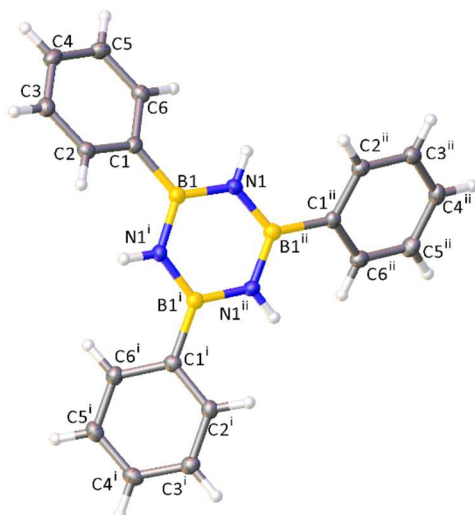


Figure S22. Structure of $[\text{HN-BPh}]_3$ with the atomic numbering scheme depicted. Ellipsoids are set at the 50% probability level. Symmetry codes $^i = 1-y, +x-y, +z$, $^{ii} = 1+y-x, 1-x, +z$. Selected bond lengths [\AA]: B1–C1 1.573(2), B1–N1 1.424(2), B1–N1ⁱ 1.425(2), N1–B1ⁱⁱ 1.425(2). Selected bond angles [$^\circ$]: N1ⁱ–B1–C1 120.92 (12), N1–B1–C1 122.36 (12), N1–B1–N1ⁱ 116.65 (14), B1–N1–B1ⁱⁱ 123.30 (14).

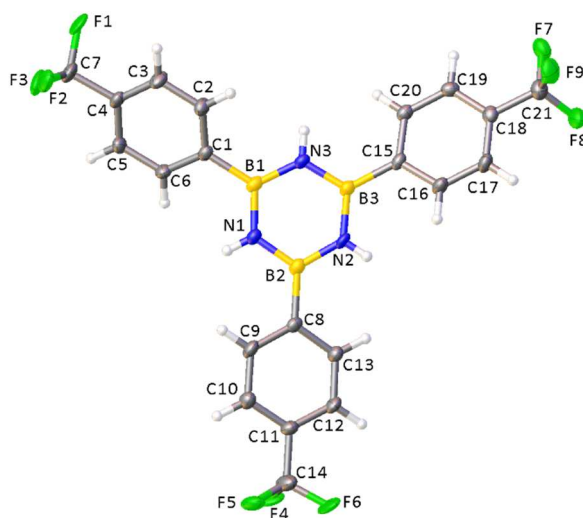


Figure S23. Structure of $[\text{HN-B}(p\text{-CF}_3\text{C}_6\text{H}_4)]_3$ with the atomic numbering scheme depicted. Ellipsoids are set at the 50% probability level. Only one orientation of the disordered CF_3 groups is shown for clarity. Selected bond lengths [\AA]: N1–B1 1.427 (4), N1–B2 1.432 (4), N2–B2 1.425 (4), N2–B3 1.426 (4), N3–B1 1.425 (4), N3–B3 1.435 (4), B1–C1 1.576 (4), B3–C15 1.571 (4), B2–C8 1.576 (4). Selected bond angles [$^\circ$]: B1–N1–B2 124.0 (3), B2–N2–B3 124.3 (2), B1–N3–B3 123.4 (2), N1–B1–C1 121.5 (3), N3–B3–C15 121.6 (2), N2–B2–C8 122.3 (2).

Table S1. Crystal data and structure refinement for [HN-BPh]₃ and [HN-B(*p*-CF₃C₆H₄)]₃.

Identification code	[HN-BPh] ₃	[HN-B(<i>p</i> -CF ₃ C ₆ H ₄)] ₃
Empirical formula	C ₁₈ H ₁₈ B ₃ N ₃	C ₂₁ H ₁₅ B ₃ F ₉ N ₃
Formula weight	308.81	512.79
Temperature/K	100(2)	100(2)
Crystal system	hexagonal	monoclinic
Space group	<i>P6cc</i>	<i>P2₁/c</i>
<i>a</i> /Å	17.1231(6)	11.0171(3)
<i>b</i> /Å	17.1231(6)	23.4105(6)
<i>c</i> /Å	7.1049(3)	8.7127(2)
<i>α</i> /°	90	90
<i>β</i> /°	90	99.1234(15)
<i>γ</i> /°	120	90
Volume/Å ³	1804.07(15)	2218.71(10)
<i>Z</i>	3.9996	4
$\rho_{\text{calc}}/\text{cm}^3$	1.137	1.535
μ/mm^{-1}	0.066	0.143
F(000)	648.0	1032.0
Crystal size/mm ³	0.637 × 0.243 × 0.204	0.59 × 0.41 × 0.25
Radiation	MoK α ($\lambda = 0.71073$)	MoK α ($\lambda = 0.71073$)
2 θ range for data collection/°	2.746 to 55.85	3.48 to 55.908
Index ranges	-22 ≤ <i>h</i> ≤ 22, -22 ≤ <i>k</i> ≤ 22, -9 ≤ <i>l</i> ≤ 9	-14 ≤ <i>h</i> ≤ 14, 0 ≤ <i>k</i> ≤ 30, 0 ≤ <i>l</i> ≤ 11
Reflections collected	38173	5313
R _{int}	0.0477	0.0408
Data/restraints/parameters	1441/1/77	5313/243/413
Goodness-of-fit on F ²	1.073	1.044
Final R indexes [<i>I</i> ≥ 2 σ (<i>I</i>)]	R ₁ = 0.0285, wR ₂ = 0.0760	R ₁ = 0.0584, wR ₂ = 0.1291
Final R indexes [all data]	R ₁ = 0.0309, wR ₂ = 0.0773	R ₁ = 0.0937, wR ₂ = 0.1482
Largest diff. peak/hole / e Å ⁻³	0.21/−0.13	0.70/−0.39

5) Dehydropolymerisation studies of $\text{NH}_3\cdot\text{BH}_2\text{Ph}$ (**1a**)

5.1 Dehydropolymerisation of **1a** using different catalysts ($[\{\text{Rh}(\text{COD})(\mu\text{-Cl})\}_2]$, $[\text{IrH}_2(\text{POCOP})]$ and skeletal nickel)

Reaction of $\text{NH}_3\cdot\text{BH}_2\text{Ph}$ (1a**) with 2.5 mol % $[\{\text{Rh}(\text{COD})(\mu\text{-Cl})\}_2]$:** To a solution of $\text{NH}_3\cdot\text{BH}_2\text{Ph}$ (53 mg, 0.5 mmol) in THF (1.0 mL) was added a solution of $[\{\text{Rh}(\text{COD})(\mu\text{-Cl})\}_2]$ (6 mg, 0.01 mmol, 2.5 mol %, 5.0 mol % Rh) in THF (1.0 mL) at 20 °C. After 6 h, an aliquot (0.4 mL) was transferred into a J. Young quartz-glass NMR tube and analysed by ^{11}B NMR spectroscopy revealing quantitative consumption of $\text{NH}_3\cdot\text{BH}_2\text{Ph}$ to yield $\text{H}_2\text{N}=\text{BPh}_2$ [δ_{B} 40.9 (s)] (*ca.* 25 %), $[\text{HN-BPh}]_3$ [δ_{B} 30.8 (br)] (*ca.* 50 %) and $[\text{NH}_2\text{-BHPH}]_n$ [δ_{B} -6.5 (br)] (*ca.* 25 %) (Figure S24).

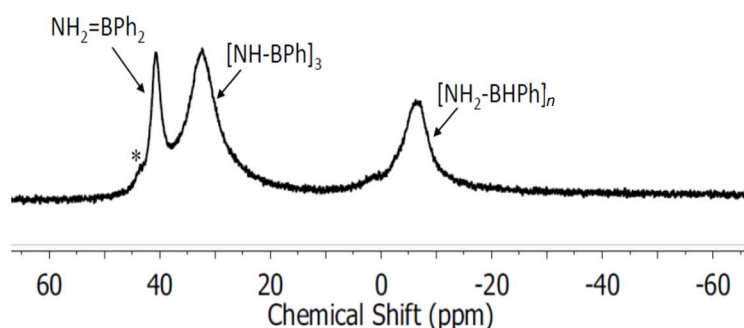


Figure S24. ^{11}B NMR spectrum of the reaction of $\text{NH}_3\cdot\text{BH}_2\text{Ph}$ (**1a**) and 2.5 mol % $[\{\text{Rh}(\text{COD})(\mu\text{-Cl})\}_2]$ in THF at 20 °C after 6 h. * Unassigned product.

Reaction of $\text{NH}_3\cdot\text{BH}_2\text{Ph}$ (1a**) with 5 mol % $[\text{IrH}_2(\text{POCOP})]$:** To a solution of $\text{NH}_3\cdot\text{BH}_2\text{Ph}$ (53 mg, 0.5 mmol) in THF (1.0 mL) was added a solution of $[\text{IrH}_2(\text{POCOP})]$ (15 mg, 0.025 mmol, 5 mol %) in THF (1.0 mL) at 20 °C. After 1 h, an aliquot (0.4 mL) was transferred into a J. Young quartz-glass NMR tube and analysed by ^{11}B NMR spectroscopy revealing quantitative consumption of $\text{NH}_3\cdot\text{BH}_2\text{Ph}$ to yield $[\text{HN-BPh}]_3$ [δ_{B} 31.6 (br)] (*ca.* 25 %) and $[\text{NH}_2\text{-BHPH}]_n$ [δ_{B} -7.2 (br)] (*ca.* 75 %) (Figure S25).

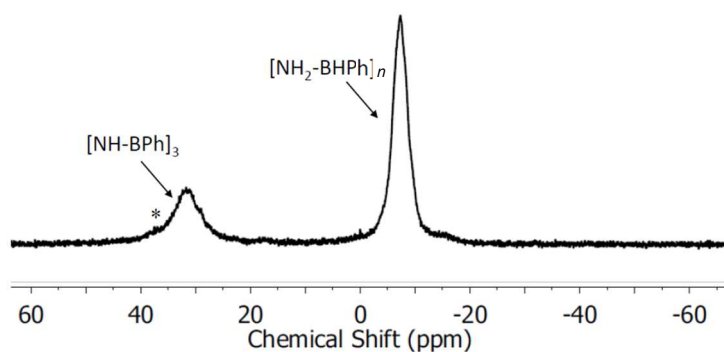


Figure S25. ^{11}B NMR spectrum of the reaction of $\text{NH}_3\cdot\text{BH}_2\text{Ph}$ (**1a**) and 5 mol % $[\text{IrH}_2(\text{POCOP})]$ in THF at 20 °C after 1 h. * Unassigned product.

Reaction of $\text{NH}_3\cdot\text{BH}_2\text{Ph}$ (1a**) with 10 mol % skeletal nickel:** To a suspension of skeletal nickel (3 mg, 0.05 mmol, 10 mol %) in THF (1.0 mL) was added a solution of $\text{NH}_3\cdot\text{BH}_2\text{Ph}$ (53 mg, 0.5 mmol) in THF (1.0 mL) at 20 °C. After 70 h, an aliquot (0.4 mL) was transferred to a J. Young quartz-glass NMR tube and analysed by ^{11}B NMR spectroscopy revealing partial consumption of $\text{NH}_3\cdot\text{BH}_2\text{Ph}$ [δ_{B} -14.0 (t, $^1J_{\text{BH}}$ = 95 Hz)] (*ca.* 50 %) to yield $[\text{HN-BPh}]_3$ [δ_{B} 32.8 (br)] (*ca.* 20 %), and $[\text{NH}_2\text{-BHPH}]_n$ [δ_{B} -6.7 (br)] (*ca.* 30 %) (Figure S26).

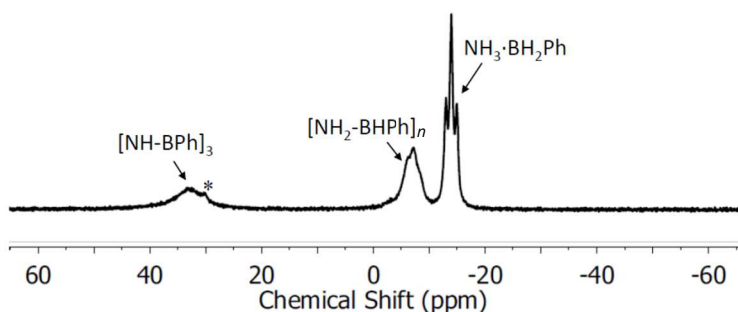


Figure S26. ^{11}B NMR spectrum of the reaction of $\text{NH}_3\cdot\text{BH}_2\text{Ph}$ (**1a**) and 10 mol % skeletal nickel in THF at 20 °C after 70 h. * Unassigned product.

Reaction of $\text{NH}_3\cdot\text{BH}_2\text{Ph}$ (1a**) with 100 mol % of skeletal nickel:** To a suspension of skeletal nickel (30 mg, 0.5 mmol) in THF (1.0 mL) was added a solution of $\text{NH}_3\cdot\text{BH}_2\text{Ph}$ (53 mg, 0.5 mmol) in THF (1.0 mL) at 20 °C. After 70 h, an aliquot (0.4 mL) was transferred to a J. Young quartz-glass NMR tube and analysed by ^{11}B NMR spectroscopy revealing quantitative consumption of $\text{NH}_3\cdot\text{BH}_2\text{Ph}$ to yield $\text{H}_2\text{N}=\text{BPh}_2$ [δ_{B} 41.0 (s)] (*ca.* 10 %), $[\text{HN-BPh}]_3$ [δ_{B} 33.1 (s)] (*ca.* 70 %) and $[\text{NH}_2\text{-BHPH}]_n$ [δ_{B} -6.5 (br)] (*ca.* 20 %) (Figure S27).

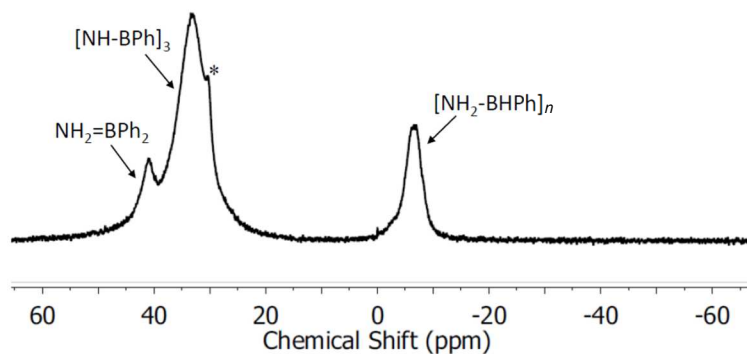


Figure S27. ^{11}B NMR spectrum of the reaction of $\text{NH}_3\cdot\text{BH}_2\text{Ph}$ (**1a**) and 100 mol % of skeletal nickel in THF at 20 °C after 70 h. * Unassigned product.

5.2 Dehydropolymerisation of **1a** with various catalyst loadings of $[\text{IrH}_2(\text{POCOP})]$

To a solution of $\text{NH}_3\cdot\text{BH}_2\text{Ph}$ (200 mg, 1.9 mmol) in THF (0.5 mL) was added a solution of $[\text{IrH}_2(\text{POCOP})]$ (0.5, 1 or 5 mol %) in THF (0.5 mL) at 20 °C. After 1 h, the solution was transferred into cold (-40 °C), stirred *n*-hexane, whereupon a colourless precipitate was observed. Excess solvent was removed via decantation and volatile byproducts removed *in vacuo* to yield an off-white solid.

Analysis of the reaction of $\text{NH}_3\cdot\text{BH}_2\text{Ph}$ (1a**) with 0.5 mol % $[\text{IrH}_2(\text{POCOP})]$ after 1 h:** ^{11}B NMR (CDCl_3): $\text{H}_2\text{N}=\text{BPh}_2$ [δ_{B} 39.2 (br)] (trace amounts), $[\text{HN-BPh}]_3$ [δ_{B} 30.2 (br)] (trace amounts), $\text{NH}_3\cdot\text{BH}_2\text{Ph}$ [δ_{B} -13.8 (t, br)] (*ca.* 80 %) and $[\text{NH}_2\text{-BHPh}]_n$ [δ_{B} -6.9 (br)] (*ca.* 20 %) (Figure S28); the GPC analysis showed the presence of a trace of high molar mass polymer in the range of 17 to 21 mL in the retention volume (Figure S29).

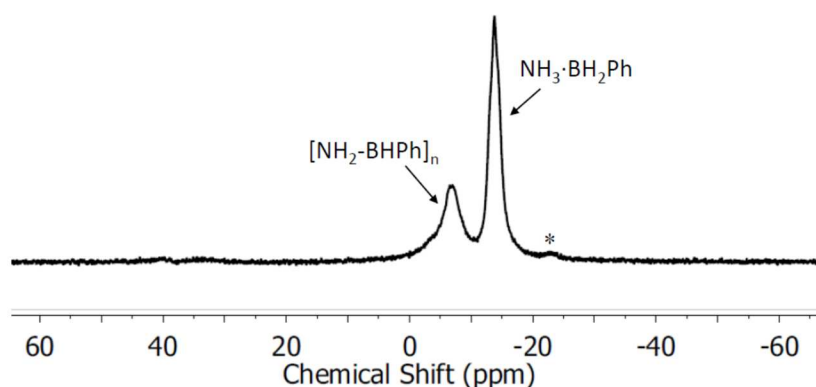


Figure S28. ^{11}B NMR spectrum of the product of the reaction of $\text{NH}_3\cdot\text{BH}_2\text{Ph}$ (**1a**) and 0.5 mol % $[\text{IrH}_2(\text{POCOP})]$ in THF at 20 °C after 1 h. * Unassigned product.

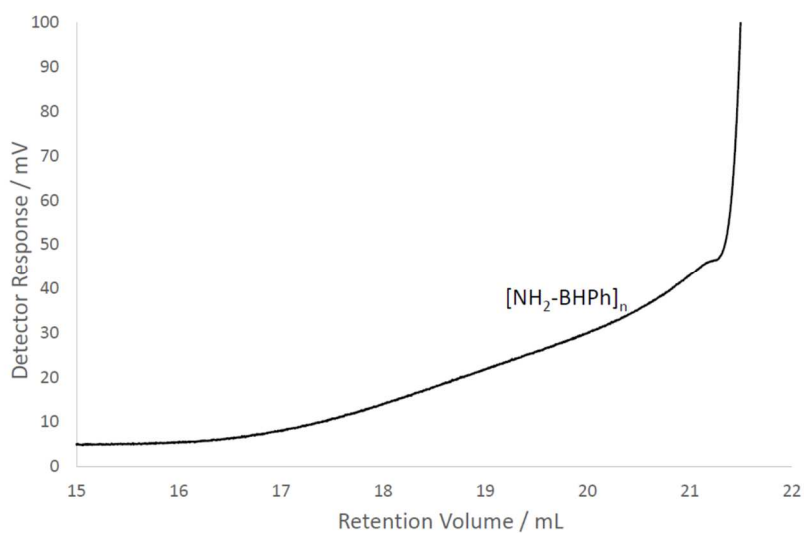


Figure S29. GPC chromatogram (2 mg mL^{-1}) of the product of the reaction of $\text{NH}_3 \cdot \text{BH}_2\text{Ph}$ (**1a**) and 0.5 mol % $[\text{IrH}_2(\text{POCOP})]$ in THF (0.1 wt% $[\text{nBu}_4\text{N}]\text{Br}$) at 20°C after 1 h.

Analysis of the reaction of $\text{NH}_3 \cdot \text{BH}_2\text{Ph}$ (1a**) with 1 mol % $[\text{IrH}_2(\text{POCOP})]$ after 1 h:** ^{11}B NMR (CDCl_3): $\text{NH}_3 \cdot \text{BH}_2\text{Ph}$ [$\delta_{\text{B}} -12.8$ (t, br)] (*ca.* 20 %) and $[\text{NH}_2\text{-BHPh}]_n$ [$\delta_{\text{B}} -6.7$ (br)] (*ca.* 80 %) (Figure S30); GPC ($M_n = 96,000 \text{ g mol}^{-1}$, $M_w = 121,000 \text{ g mol}^{-1}$, PDI = 1.25) (Figure S31).

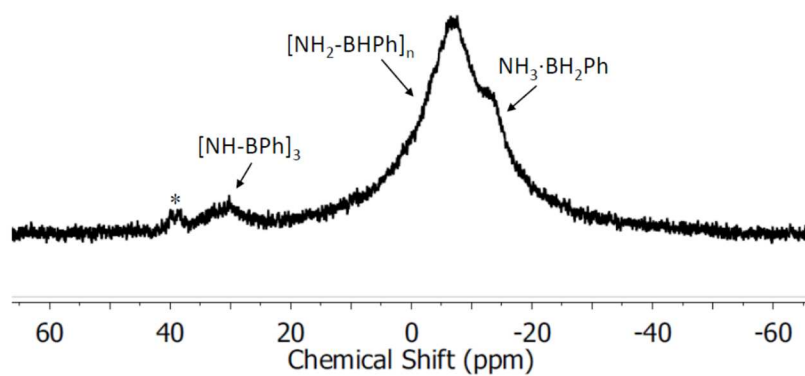


Figure S30. ^{11}B NMR spectrum of the product of the reaction of $\text{NH}_3 \cdot \text{BH}_2\text{Ph}$ (**1a**) and 1 mol % $[\text{IrH}_2(\text{POCOP})]$ in THF at 20°C after 1 h. * Unassigned product.

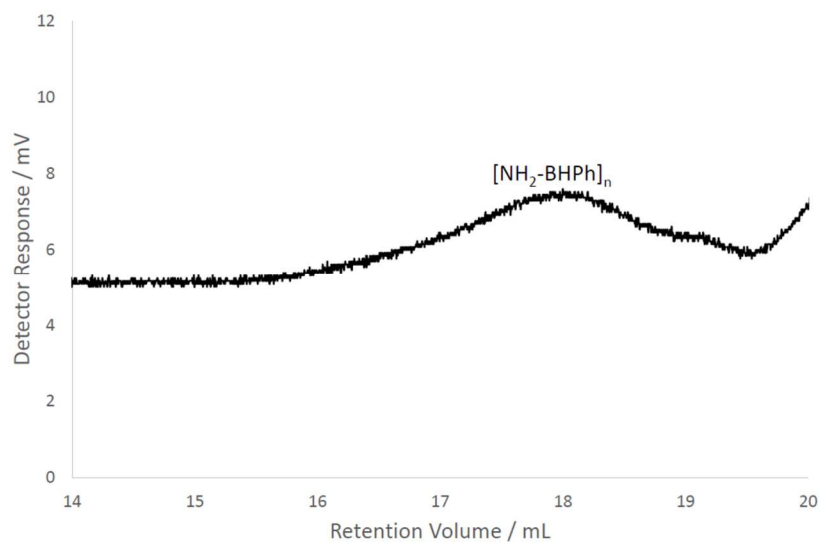


Figure S31. GPC chromatogram (2 mg mL^{-1}) of the product of the reaction of $\text{NH}_3\cdot\text{BH}_2\text{Ph}$ (**1a**) and 1 mol % $[\text{IrH}_2(\text{POCOP})]$ in THF (0.1 wt% $[\text{nBu}_4\text{N}]\text{Br}$) at 20°C after 1 h.

Analysis of the reaction of $\text{NH}_3\cdot\text{BH}_2\text{Ph}$ (1a**) with 5 mol % $[\text{IrH}_2(\text{POCOP})]$ after 1 h:** ^{11}B NMR (CDCl_3): $[\text{HN-BPh}]_3$ [δ_{B} 31.4 (br)] (trace amounts), $[\text{NH}_2\text{-BHPh}]_n$ [δ_{B} -6.0 (d, br)] (Figure S32); GPC ($M_{\text{n}} = 97,000 \text{ g mol}^{-1}$, $M_{\text{w}} = 112,000 \text{ g mol}^{-1}$, PDI = 1.16) (Figure S33).

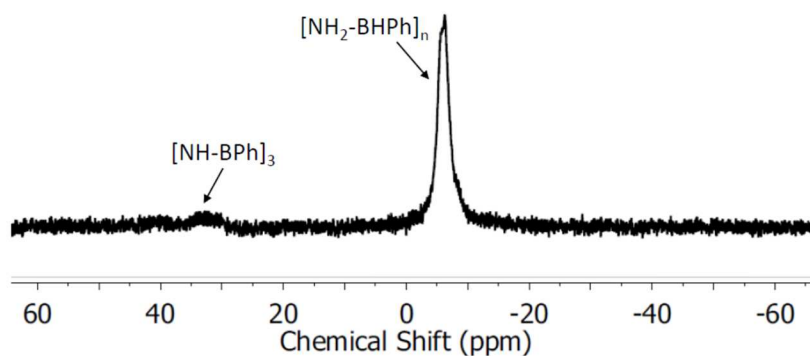


Figure S32. ^{11}B NMR spectrum of the product of the reaction of $\text{NH}_3\cdot\text{BH}_2\text{Ph}$ (**1a**) and 5 mol % $[\text{IrH}_2(\text{POCOP})]$ in THF at 20°C after 1 h.

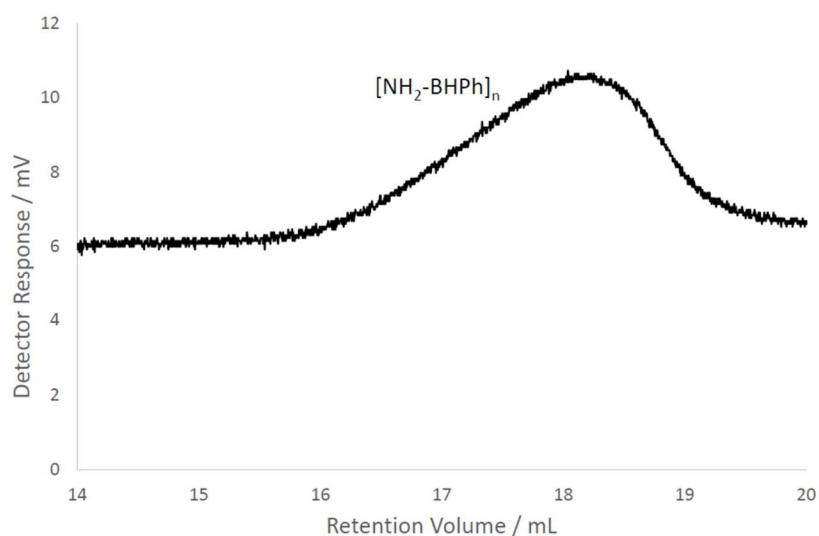


Figure S33. GPC chromatogram (2 mg mL^{-1}) of the product of the reaction of $\text{NH}_3\cdot\text{BH}_2\text{Ph}$ (**1a**) and 5 mol % $[\text{IrH}_2(\text{POCOP})]$ in THF (0.1 wt% $[\text{nBu}_4\text{N}]\text{Br}$) at 20°C after 1 h.

5.3 Dehydropolymerisation of **1a** with 1 mol % $[\text{IrH}_2(\text{POCOP})]$ after various reaction times

To a solution of $\text{NH}_3\cdot\text{BH}_2\text{Ph}$ (200 mg, 1.9 mmol) in THF (0.5 mL) was added a solution of $[\text{IrH}_2(\text{POCOP})]$ (1 mol %) in THF (0.5 mL) at 20°C . After 0.5 or 2 h, the solution was transferred into cold (-40°C), stirred *n*-hexane, whereupon a colourless precipitate was observed. Excess solvent was removed via decantation and volatile byproducts were removed *in vacuo*.

Analysis of the reaction of $\text{NH}_3\cdot\text{BH}_2\text{Ph}$ (1a**) with 1 mol % $[\text{IrH}_2(\text{POCOP})]$ after 0.5 h:** ^{11}B NMR (CDCl_3): $\text{H}_2\text{NH}=\text{BPh}_2$ [δ_{B} 40.2 (br)] (trace amounts), $[\text{HN-BPh}]_3$ [δ_{B} 31.8 (br)] (trace amounts), $\text{NH}_3\cdot\text{BH}_2\text{Ph}$ [δ_{B} -13.4 (t, br)] (*ca.* 20 %) and $[\text{NH}_2\text{-BPh}]_n$ [δ_{B} -6.9 (br)] (*ca.* 80 %) (Figure S34); GPC ($M_n = 30,000 \text{ g mol}^{-1}$, $M_w = 63,000 \text{ g mol}^{-1}$, PDI = 2.11) (Figure S35).

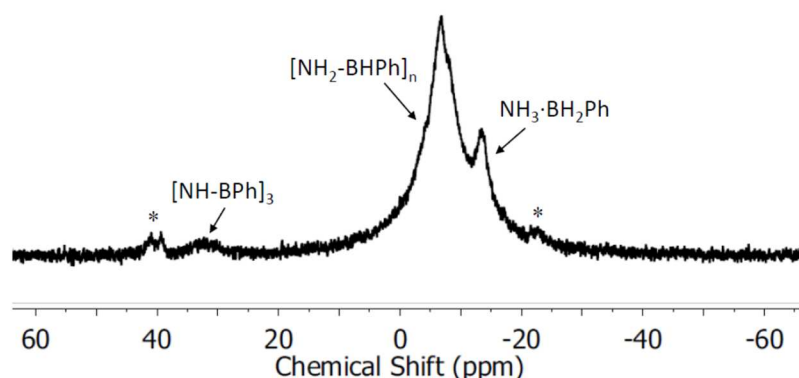


Figure S34. ^{11}B NMR spectrum of the product of the reaction of $\text{NH}_3\cdot\text{BH}_2\text{Ph}$ (**1a**) and 1 mol % $[\text{IrH}_2(\text{POCOP})]$ in THF at 20°C after 0.5 h. * Unassigned product.

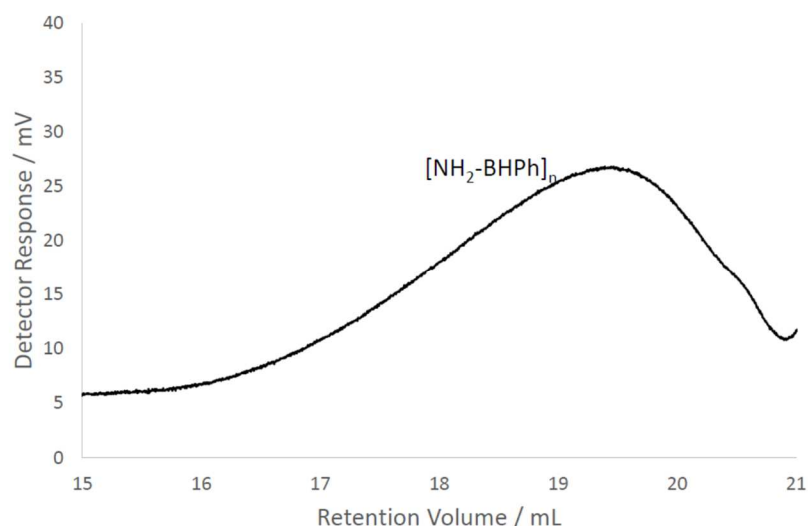


Figure S35. GPC chromatogram (2 mg mL^{-1}) of the product of the reaction of $\text{NH}_3\cdot\text{BH}_2\text{Ph}$ (**1a**) and 1 mol % $[\text{IrH}_2(\text{POCOP})]$ in THF (0.1 wt% $[\text{nBu}_4\text{N}]\text{Br}$) at 20°C after 0.5 h.

Analysis of the reaction of $\text{NH}_3\cdot\text{BH}_2\text{Ph}$ (1a**) with 1 mol % $[\text{IrH}_2(\text{POCOP})]$ after 2 h:** ^{11}B NMR (CDCl_3): $\text{H}_2\text{N}=\text{BPh}_2$ [δ_{B} 41.2 (br)] (trace amounts), $[\text{HN-BPh}]_3$ [δ_{B} 33.3 (br)], $\text{NH}_3\cdot\text{BH}_2\text{Ph}$ [δ_{B} -13.4 (t, br)] (*ca.* 20 %) and $[\text{NH}_2\text{-BHPh}]_n$ [δ_{B} -4.0 (br)] (*ca.* 80 %) (Figure S36); GPC ($M_n = 41,000 \text{ g mol}^{-1}$, $M_w = 89,000 \text{ g mol}^{-1}$, PDI = 2.15) (Figure S37).

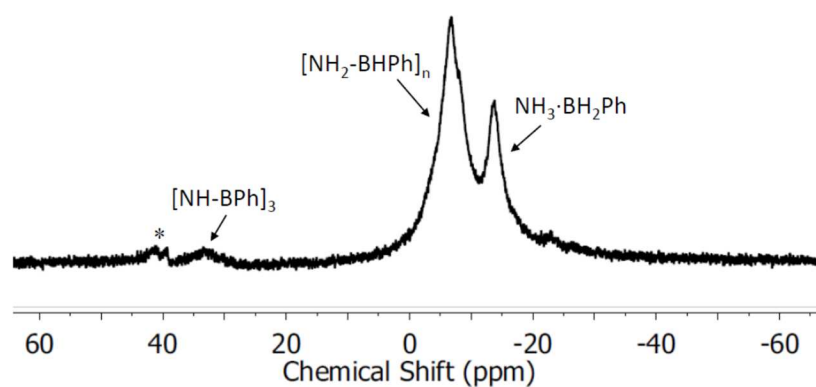


Figure S36. ^{11}B NMR spectrum of the product of the reaction of $\text{NH}_3\cdot\text{BH}_2\text{Ph}$ (**1a**) and 1 mol % $[\text{IrH}_2(\text{POCOP})]$ in THF at 20°C after 2 h. * Unassigned product.

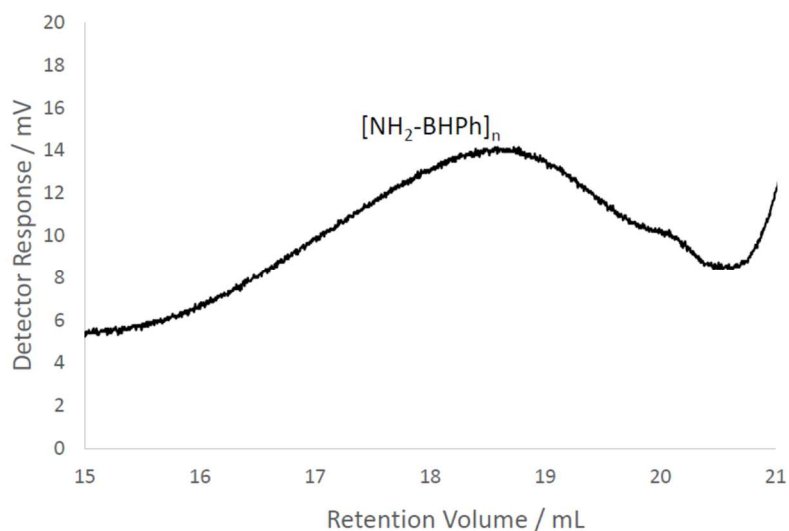


Figure S37. GPC chromatogram (2 mg mL^{-1}) of the product of the reaction of $\text{NH}_3 \cdot \text{BH}_2\text{Ph}$ (**1a**) and 1 mol % $[\text{IrH}_2(\text{POCOP})]$ in THF (0.1 wt% $[\text{nBu}_4\text{N}]\text{Br}$) at $20 \text{ }^\circ\text{C}$ after 2 h.

Table S2: Influence of different catalyst loadings of $[\text{IrH}_2(\text{POCOP})]$ and reaction times on the dehydropolymerisation of **1a** in THF at $20 \text{ }^\circ\text{C}$.

Catalyst loading [mol %]	Reaction time [h]	Conversion [%] ^a	$M_n / [\text{g mol}^{-1}]^b$	PDI ^b
0.5	1	30	— ^c	— ^c
1	1	80	96,000	1.25
5	1	100	97,000	1.16
1	0.5	80	30,000	2.11
1	2	80	41,000	2.15

^a determined by integration of the signals in the ^{11}B NMR spectra of the reaction mixtures. ^b

determined by GPC analysis of the isolated solids in THF (2 mg mL^{-1}) containing 0.1 wt% $[\text{nBu}_4\text{N}]\text{Br}$.

^c the GPC analysis showed that only a trace of high molecular weight material was present.

6) Synthesis and Characterisation of poly(*B*-aryl aminoboranes)

6.1 Synthesis and Characterisation of [NH₂-BHPPh]_{*n*} (**2a**)

To a solution of NH₃·BH₂Ph (300 mg, 2.8 mmol) in THF (0.5 mL) was added a solution of [IrH₂(POCOP)] (83 mg, 0.14 mmol, 5 mol %) in THF (0.5 mL) at 20 °C. After 1 h, the solution was transferred into cold (−40 °C) stirred *n*-hexane, whereupon formation of a colourless precipitate was observed. Excess solvent was removed via decantation and the solid was re-precipitated using a minimal amount of CH₂Cl₂ (*ca.* 0.5 mL) and excess *n*-hexane (*ca.* 15 mL). Decantation was then repeated. Residual solvent and volatile byproducts were removed *in vacuo* to yield a colourless solid. Yield: 115 mg (1.1 mmol, 38 %).

¹¹B NMR (THF): δ_B −7.4 (br). Trace amounts of unassigned peaks were observed at [δ_B 39.5 (br)] and [δ_B 30.4 (br)] (Figure S38).

¹H NMR (CDCl₃): δ_H 7.12 (5 H, m, br, ArH), 2.55 (3 H, s, br, BH, NH) (Figure S39).

GPC: *M*_n = 81,600 g mol^{−1}, *M*_w = 108,700 g mol^{−1}, PDI = 1.33 (Figure S40).

ESI-MS: Difference of 105 *m/z* ([NH₂-BHPPh] subunit) confirms presence of linear oligo(*B*-phenyl aminoborane) **2a** up to 14 repeat units (Figure S41).

TGA: A sample of solid [NH₂-BHPPh]_{*n*} showed thermal stability up to *ca.* 60 °C, whereupon gradual weight loss occurred until *ca.* 275 °C and *ca.* 5 wt. % remained up to 600 °C (Figure S42).

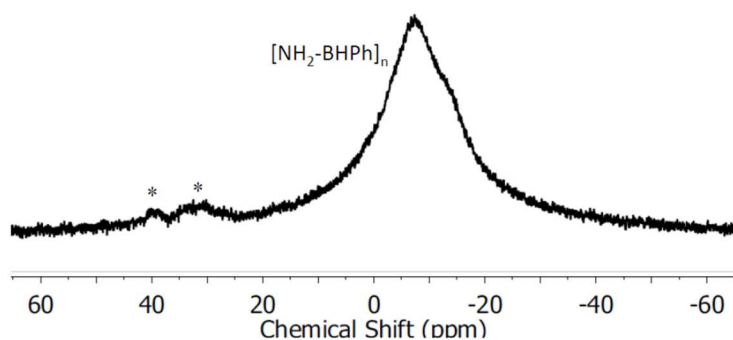


Figure S38. ¹¹B NMR spectrum of isolated [NH₂-BHPPh]_{*n*} (**2a**) in THF-d₈ at 20 °C. * Unassigned product.

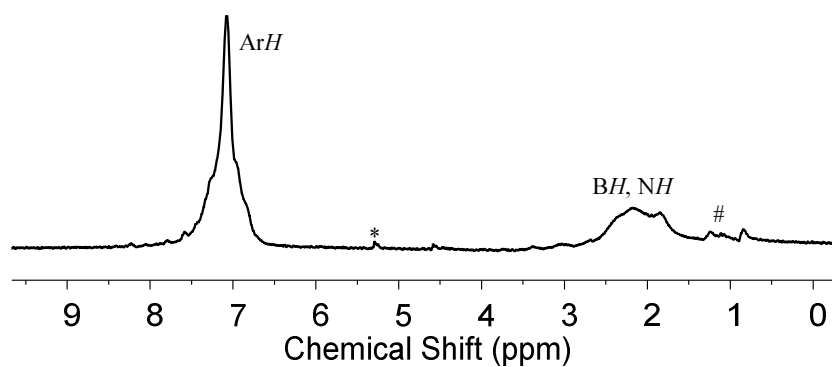


Figure S39. ^1H NMR spectrum of isolated $[\text{NH}_2\text{-BHPH}]_n$ (**2a**) in CD_2Cl_2 . * CD_2Cl_2 , # *n*-hexane.

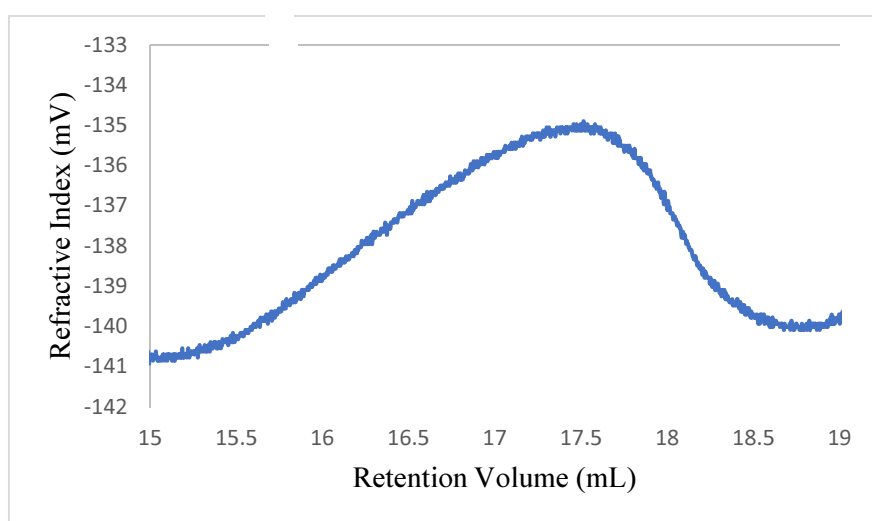


Figure S40. GPC chromatogram (2 mg mL^{-1}) of isolated $[\text{NH}_2\text{-BHPH}]_n$ (**2a**) in THF (0.1 wt% $[\text{nBu}_4\text{N}]\text{Br}$).

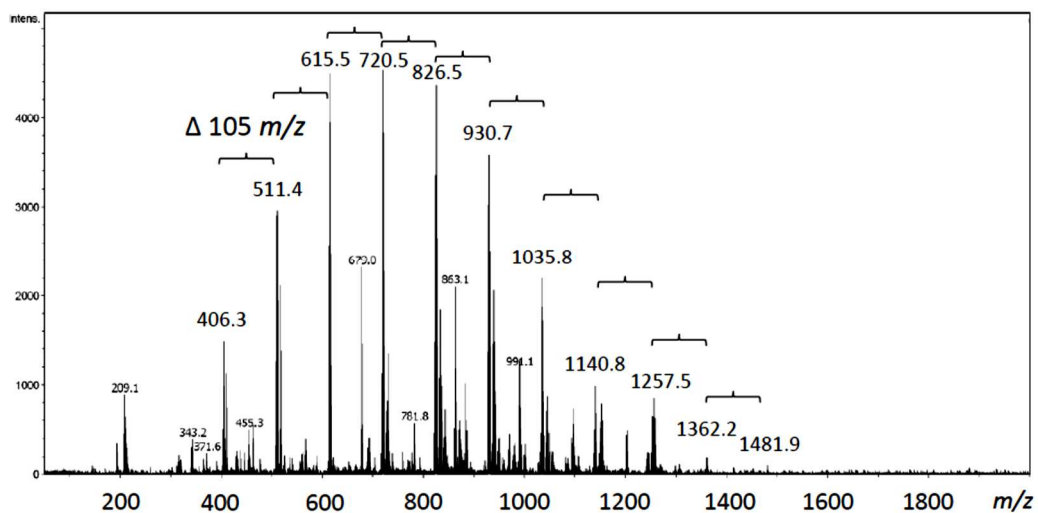


Figure S41. ESI mass spectrum of isolated $[\text{NH}_2\text{-BHPh}]_n$ (**2a**) in THF, leading to the detection of an oligomeric fraction of up to 14 subunits.

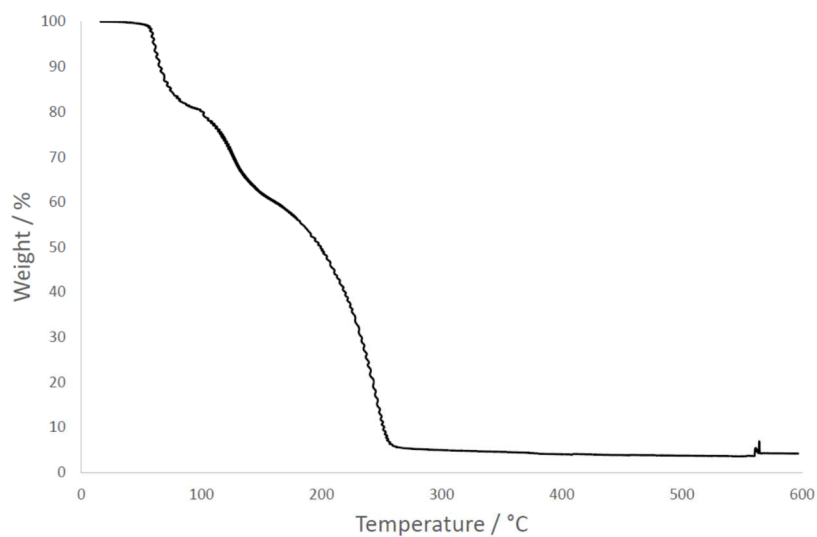


Figure S42. TGA plot of isolated $[\text{NH}_2\text{-BHPh}]_n$ (**2a**) (heating rate: 10 °Cmin^{-1} , N_2 gas flow).

6.2 Synthesis and characterisation of $[\text{NH}_2\text{-BH}(p\text{-CF}_3\text{C}_6\text{H}_4)]_n$ (**2b**)

To a solution of $\text{NH}_3\cdot\text{BH}_2(p\text{-CF}_3\text{C}_6\text{H}_4)$ (300 mg, 1.71 mmol) in a mixture of THF (0.2 mL) and toluene (0.8 mL) was added $[\text{IrH}_2(\text{POCOP})]$ (51 mg, 0.086 mmol, 5 mol %) at 20 °C. After 1 h, the solution was transferred into cold (-40 °C), stirred *n*-hexane, whereupon formation of a colourless precipitate was observed. Excess solvent was removed via decantation and the solid was re-precipitated using a minimal amount of CH_2Cl_2 (*ca.* 0.5 mL) and excess *n*-hexane (*ca.* 15 mL). Decantation was then repeated. Residual solvent and volatile byproducts were removed *in vacuo* to yield a colourless solid. Yield: 120 mg (0.69 mmol, 40 %).

^{11}B NMR (96 MHz, CD_2Cl_2): δ_{B} -7.8 (br) (Figure S43).

^1H NMR (400 MHz, CD_2Cl_2): δ_{H} 7.25-6.86 (4 H, m, br, *ortho*-ArH, *meta*-ArH), 2.16 (3 H, s, br, BH, NH) (Figure S44).

$^{19}\text{F}\{^1\text{H}\}$ NMR (376 MHz, CD_2Cl_2): δ = -62.9 (s) (Figure S45).

GPC: M_n = 86,800 g mol⁻¹, M_w = 119,400 g mol⁻¹, PDI = 1.37 (Figure S46).

ESI-MS: Difference of 173 *m/z* ($[\text{NH}_2\text{-BH}(p\text{-CF}_3\text{C}_6\text{H}_4)]$ subunit) confirms presence of linear oligo(*B*-aryl aminoborane) **2b** up to 8 repeat units (Figure S47).

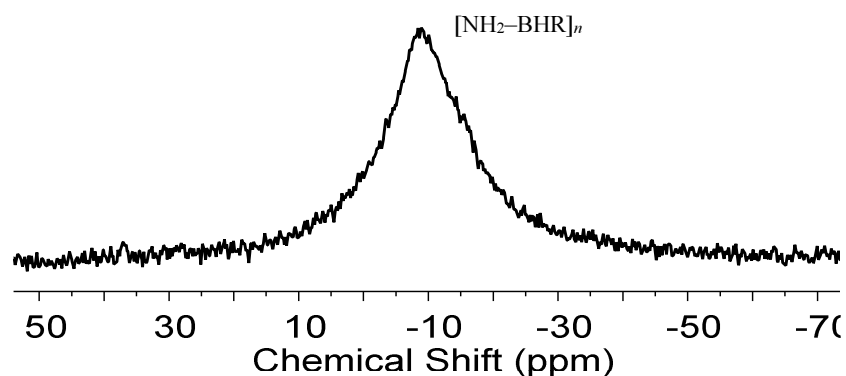


Figure S43. ^{11}B NMR spectrum of isolated $[\text{NH}_2\text{-BH}(p\text{-CF}_3\text{C}_6\text{H}_4)]_n$ (**2b**) in CD_2Cl_2 at 20 °C. R = *p*- $\text{CF}_3\text{C}_6\text{H}_4$.

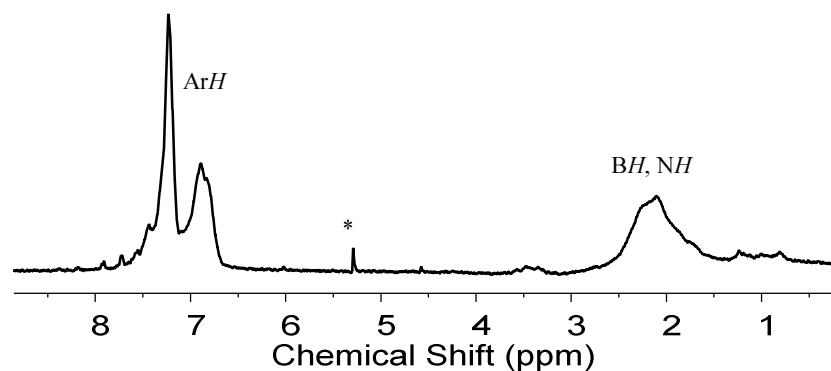


Figure S44. ^1H NMR spectrum of isolated $[\text{NH}_2\text{-BH}(p\text{-CF}_3\text{C}_6\text{H}_4)]_n$ (**2b**) in CD_2Cl_2 at 20°C . * CD_2Cl_2 .

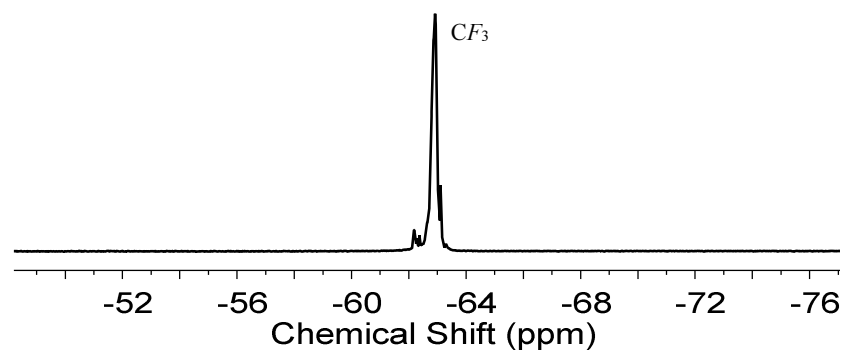


Figure S45. $^{19}\text{F}\{^1\text{H}\}$ NMR spectrum of isolated $[\text{NH}_2\text{-BH}(p\text{-CF}_3\text{C}_6\text{H}_4)]_n$ (**2b**) in CD_2Cl_2 at 20°C .

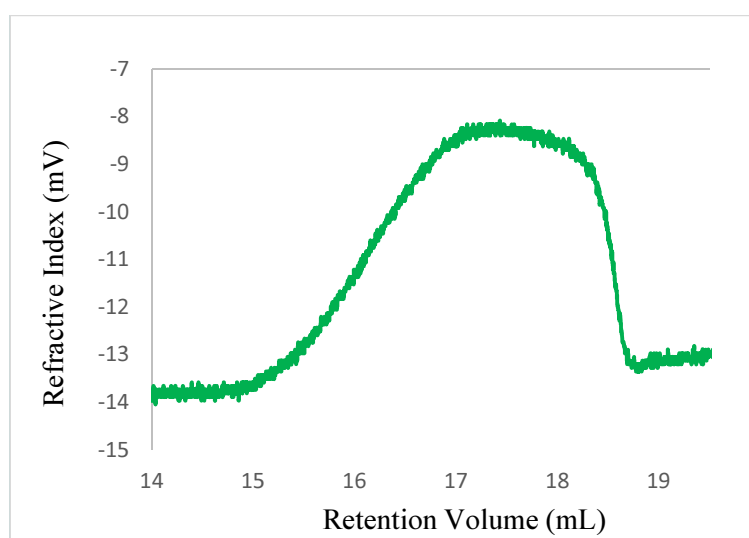


Figure S46. GPC chromatogram (2 mg mL^{-1}) of isolated $[\text{NH}_2\text{-BH}(p\text{-CF}_3\text{C}_6\text{H}_4)]_n$ (**2b**) in THF ($0.1\text{ wt}\%$ $[\text{nBu}_4\text{N}]\text{Br}$).

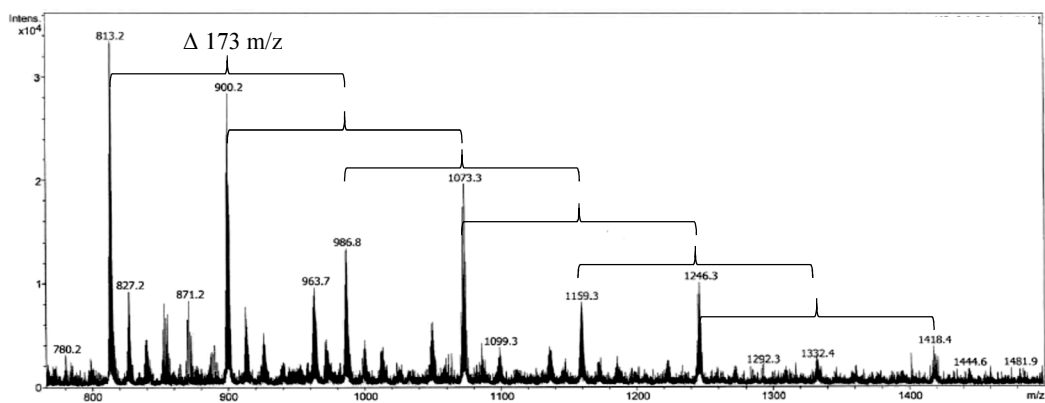


Figure S47. ESI mass spectrum of isolated $[\text{NH}_2\text{-BH}(p\text{-CF}_3\text{C}_6\text{H}_4)]_n$ (**2b**) in CH_3CN , leading to the detection of an oligomeric fraction of up to 8 subunits.

6.3 GPC analysis of 2a and 2b at different concentrations

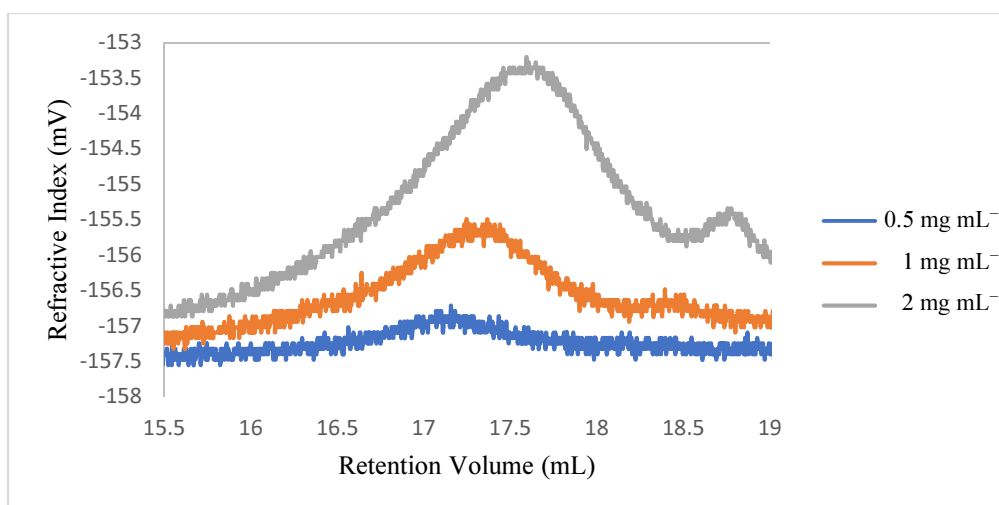


Figure S48. GPC chromatograms of $[\text{NH}_2\text{-BHPH}]_n$ (**2a**) in THF (0.1 wt% $[\text{nBu}_4\text{N}]\text{Br}$) at different concentrations. Note: another batch of polymer was used for the measurement, which was synthesised following exactly the procedure described in section 6.1. Samples were prepared using pure THF.

Table S3: Number average molecular weight (M_n), mass average molecular weight (M_w) and polydispersity index (PDI) for $[\text{NH}_2\text{-BHPH}]_n$ (**2a**) at different concentrations (c).

c (mg mL^{-1})	M_n (g mol^{-1})	M_w (g mol^{-1})	PDI
0.5	98,800	120,700	1.22
1	82,400	102,200	1.24
2	73,900	91,700	1.24

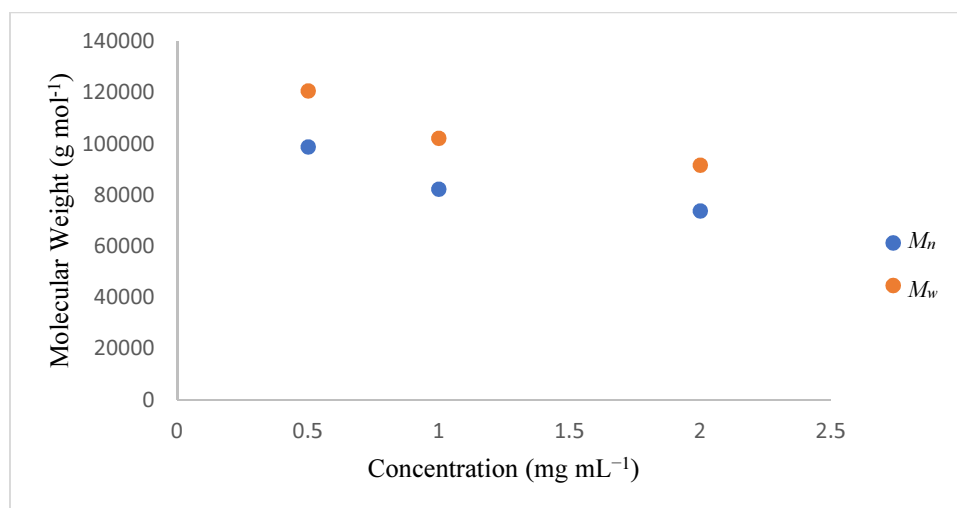


Figure S49. Plot of the molecular weight of $[\text{NH}_2\text{-BHPH}]_n$ (**2a**) versus the concentration in THF.

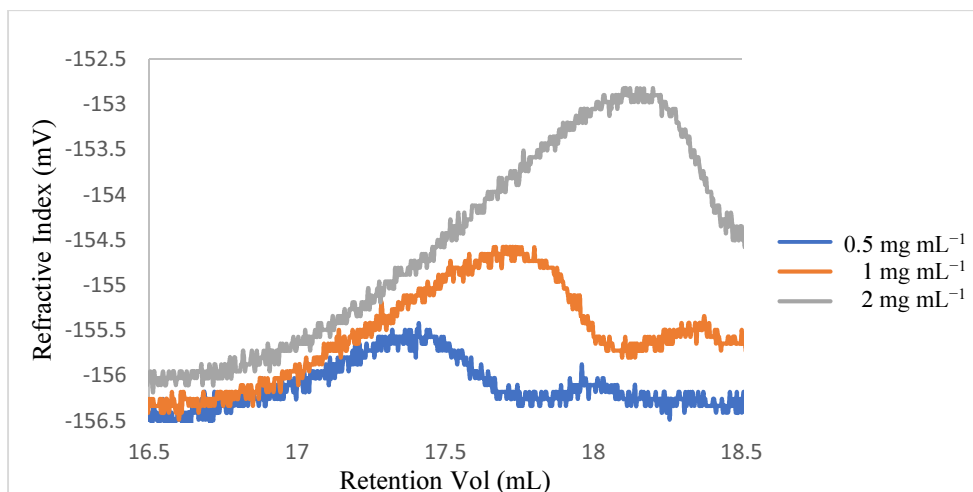


Figure S50. GPC chromatograms of $[\text{NH}_2\text{-BH}(p\text{-CF}_3\text{C}_6\text{H}_4)]_n$ (**2b**) in THF (0.1 wt% $[\text{nBu}_4\text{N}]\text{Br}$) at different concentrations. Note: another batch of polymer was used for the measurement, which was synthesised following exactly the procedure described in section 6.2. Samples were prepared using pure THF.

Table S4: Number average molecular weight (M_n), mass average molecular weight (M_w) and polydispersity index (PDI) for $[\text{NH}_2\text{-BH}(p\text{-CF}_3\text{C}_6\text{H}_4)]_n$ (**2b**) at different concentrations (c).

c (mg mL^{-1})	M_n (g mol^{-1})	M_w (g mol^{-1})	PDI
0.5	75,900	84,000	1.11
1	53,300	64,900	1.21
2	36,900	50,500	1.63

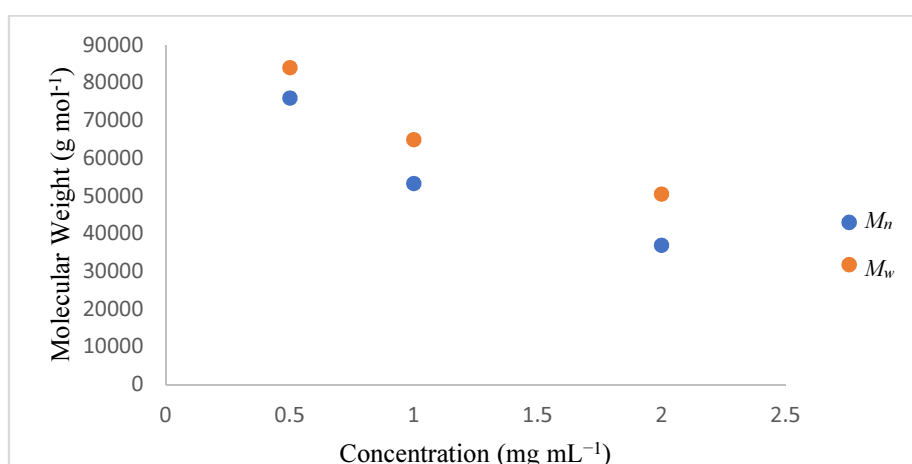


Figure S51. Plot of the molecular weight of $[\text{NH}_2\text{-BH}(p\text{-CF}_3\text{C}_6\text{H}_4)]_n$ (**2b**) versus the concentration in THF.

6.4 DLS analysis of 2a and 2b

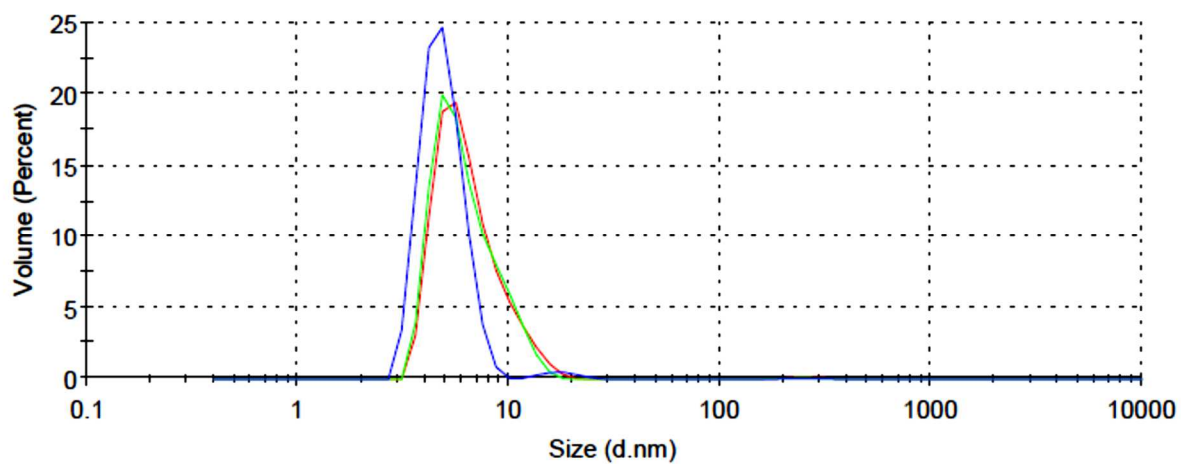


Figure S52. DLS (size distribution by volume, repeat scans) of **(2a)** (2 mg mL^{-1}) in DCM [$R_H = 2.5 \text{ nm}$ (average value)].

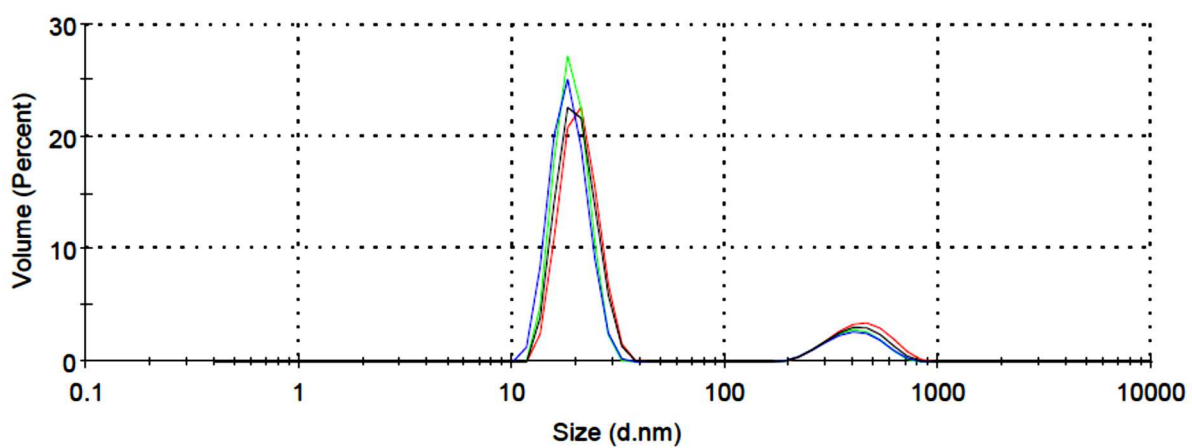


Figure S53. DLS (size distribution by volume, repeat scans) of **(2b)** (2 mg mL^{-1}) in DCM [$R_H = 10.1 \text{ nm}$ (average value)].

7) Thermal studies of $[\text{NH}_2\text{-BPh}]_n$ (**2a**) and $[\text{NH}_2\text{-BH}(p\text{-CF}_3\text{C}_6\text{H}_4)]_n$ (**2b**)

7.1 Thermal studies in the solid State

Thermal stability of solid $[\text{NH}_2\text{-BPh}]_n$ (2a**) at 20 °C:** Solid $[\text{NH}_2\text{-BPh}]_n$ (26 mg, 0.25 mmol) was allowed to stand at 20 °C. After 170 h, the solid was dissolved in THF (0.4 mL) and analysed by ^{11}B NMR spectroscopy to reveal partial consumption of $[\text{NH}_2\text{-BPh}]_n$ [δ_{B} -6.8 (br)] (*ca.* 60 %) to yield $\text{H}_2\text{N=BPh}_2$ [δ_{B} 41.1 (br)] (*ca.* 5 %), $[\text{HN-BPh}]_3$ [δ_{B} 32.7 (br)] (*ca.* 10 %) and $\text{NH}_3\cdot\text{BH}_2\text{Ph}$ [δ_{B} -13.5 (br)] (*ca.* 25 %) (Figure S54). Analysis of the solution by GPC confirmed the presence of high molecular weight polymer ($M_n = 77,000 \text{ g mol}^{-1}$, $M_w = 102,000 \text{ g mol}^{-1}$, PDI = 1.32) (Figure S55).

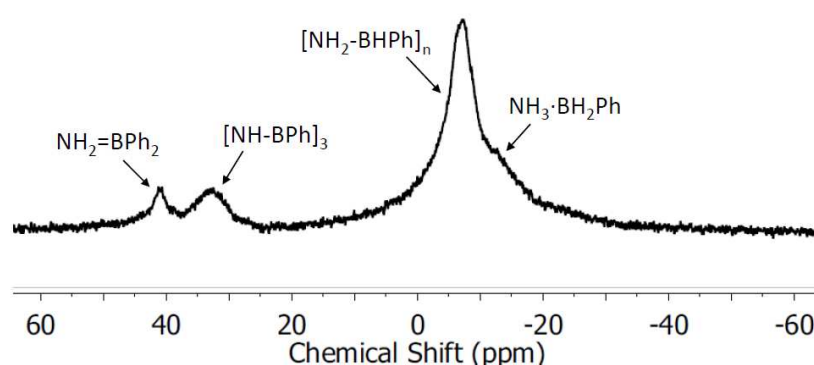


Figure S54. ^{11}B NMR spectrum of $[\text{NH}_2\text{-BPh}]_n$ (**2a**) in THF after leaving as a solid at 20 °C for 170 h.

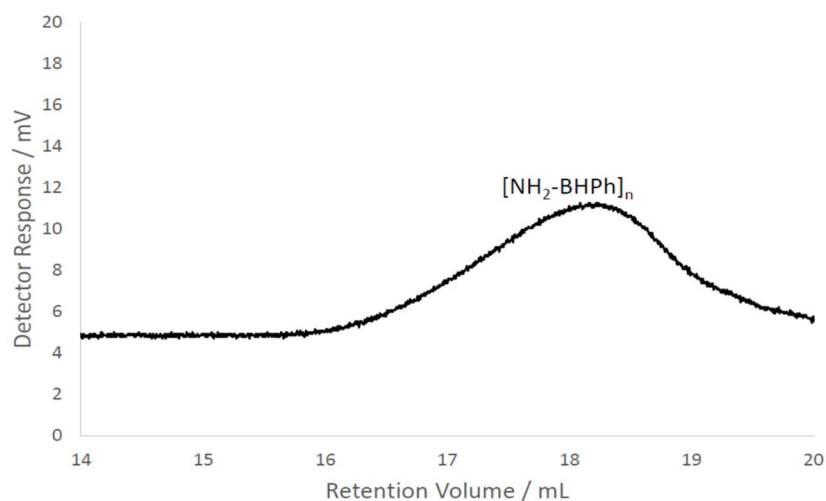


Figure S55. GPC chromatogram (2 mg mL^{-1}) of $[\text{NH}_2\text{-BPh}]_n$ (**2a**) in THF (0.1 wt% $[\text{nBu}_4\text{N}]\text{Br}$) after leaving as a solid at 20 °C for 170 h.

Thermal stability of solid $[\text{NH}_2\text{-BPh}]_n$ (2a**) at 70 °C:** Solid $[\text{NH}_2\text{-BPh}]_n$ (26 mg, 0.25 mmol) was heated to 70 °C for 24 h. After cooling to 20 °C, the solid was dissolved in THF (0.4 mL). Analysis by ^{11}B NMR spectroscopy revealed quantitative consumption of $[\text{NH}_2\text{-BPh}]_n$ [δ_{B} -6.3 (br)] (trace amounts) to yield $[\text{HN-BPh}]_3$ [δ_{B} 33.5 (br)] as the sole product (Figure S56).

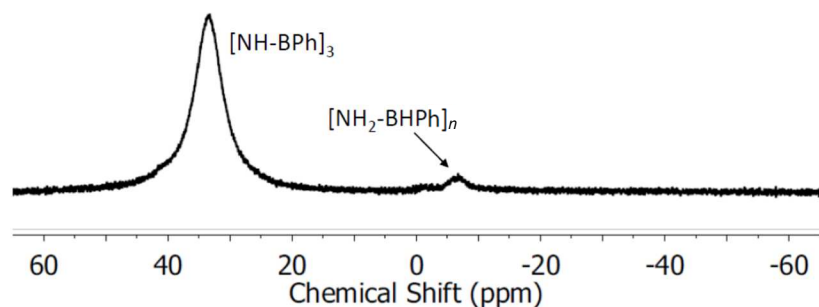


Figure S56. ^{11}B NMR spectrum of $[\text{NH}_2\text{-BPh}]_n$ (**2a**) in THF after heating as a solid at 70 °C for 170 h.

Thermal stability of solid $[\text{NH}_2\text{-BH}(p\text{-CF}_3\text{C}_6\text{H}_4)]_n$ (2b**):** Solid $[\text{NH}_2\text{-BH}(p\text{-CF}_3\text{C}_6\text{H}_4)]_n$ (43 mg, 0.25 mmol) was allowed to stand at 20 °C. After 170 h, the solid was dissolved in THF (0.4 mL) and analysed by ^{11}B NMR spectroscopy to reveal no change of $[\text{NH}_2\text{-BH}(p\text{-CF}_3\text{C}_6\text{H}_4)]_n$ [δ_{B} -8.8 (br)] (Figure S57). Analysis of the solution by GPC confirmed the presence of high molecular weight polymer ($M_n = 123,900 \text{ g mol}^{-1}$, $M_w = 157,500 \text{ g mol}^{-1}$, PDI = 1.27). (Figure S58)

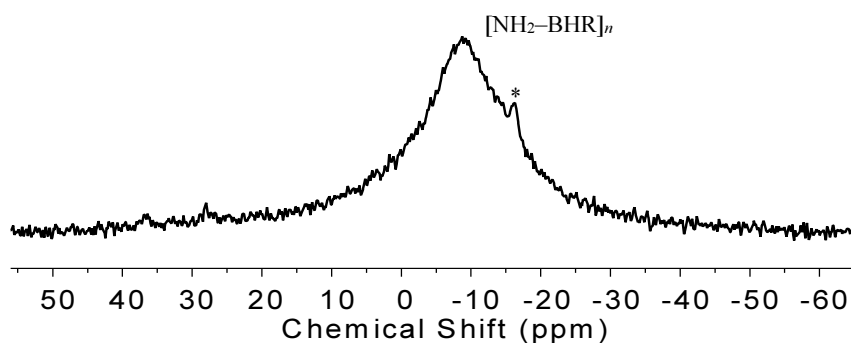


Figure S57. ^{11}B NMR spectrum of $[\text{NH}_2\text{-BH}(p\text{-CF}_3\text{C}_6\text{H}_4)]_n$ (**2b**) in THF after leaving as a solid at 20 °C for 170 h. R = $p\text{-CF}_3\text{C}_6\text{H}_4$. * Traces of $\text{NH}_3\cdot\text{BH}_2(p\text{-CF}_3\text{C}_6\text{H}_4)$.

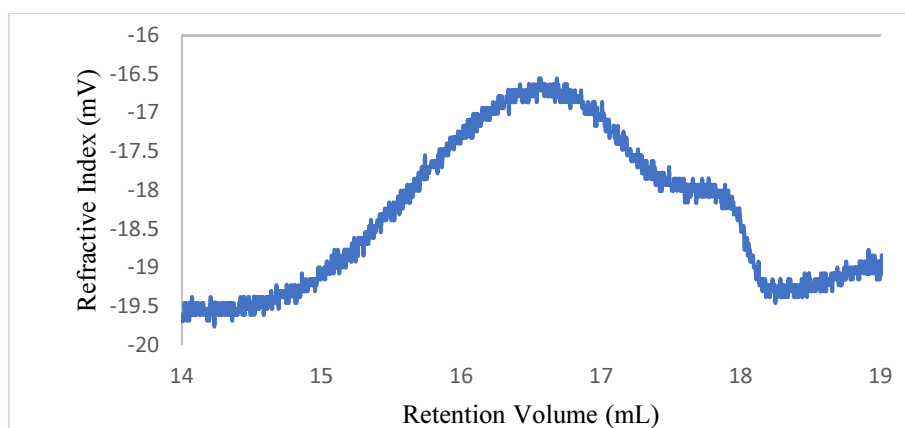


Figure S58. GPC chromatogram (2 mg mL^{-1}) of $[\text{NH}_2\text{-BH}(p\text{-CF}_3\text{C}_6\text{H}_4)]_n$ (**2b**) in THF (0.1 wt% $[\text{nBu}_4\text{N}]\text{Br}$) after leaving as a solid at 20°C for 170 h.

Thermal stability of solid $[\text{NH}_2\text{-BH}(p\text{-CF}_3\text{C}_6\text{H}_4)]_n$ (2b**) at 70°C :** Solid $[\text{NH}_2\text{-BH}(p\text{-CF}_3\text{C}_6\text{H}_4)]_n$ (88 mg, 0.25 mmol) was heated to 70°C for 170 h. After cooling to 20°C , the residue was dissolved in THF (0.4 mL). Analysis by ^{11}B NMR spectroscopy revealed partial consumption of $[\text{NH}_2\text{-BH}(p\text{-CF}_3\text{C}_6\text{H}_4)]_n$ [$\delta_{\text{B}} -7.4$ (br)] (ca. 60%) to yield an unknown product at [$\delta_{\text{B}} 12.3$ (br)] (ca. 40%) and trace amounts of $[\text{HN-B}(p\text{-CF}_3\text{C}_6\text{H}_4)]_3$ [$\delta_{\text{B}} 29.3$ (br)] (Figure S59). Analysis of the solution by GPC confirmed the presence of high molecular weight material ($M_n = 77,500 \text{ g mol}^{-1}$, $M_w = 81,000 \text{ g mol}^{-1}$, PDI = 1.04) (Figure S60).

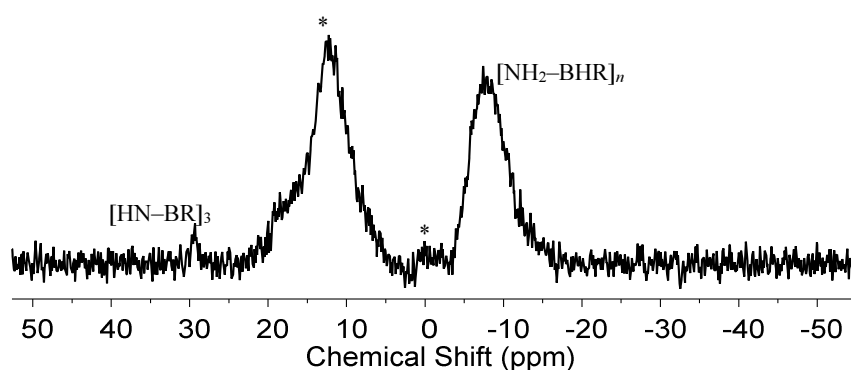


Figure S59. ^{11}B NMR spectrum of $[\text{NH}_2\text{-BH}(p\text{-CF}_3\text{C}_6\text{H}_4)]_n$ (**2b**) in THF after heating as a solid at 70°C for 170 h. * Unknown species. R = $p\text{-CF}_3\text{C}_6\text{H}_4$.

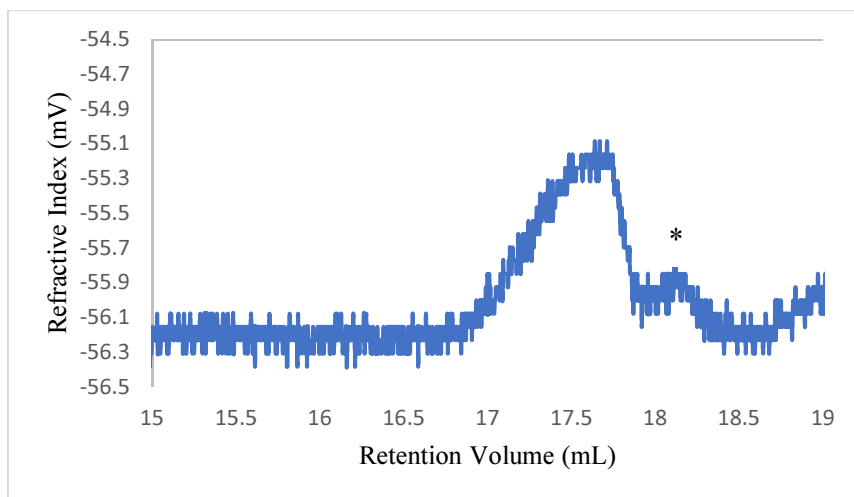


Figure S60. GPC chromatogram (2 mg mL^{-1}) of $[\text{NH}_2\text{-BH}(p\text{-CF}_3\text{C}_6\text{H}_4)]_n$ (**2b**) in THF (0.1 wt% $[\text{nBu}_4\text{N}]\text{Br}$) after heating as a solid at $70 \text{ }^\circ\text{C}$ for 170 h. The asterisk (*) marks an additional trace, which was present in the polymer batch used for the thermal studies.

7.2 Thermal Studies in Solution

Thermal stability $[\text{NH}_2\text{-BHPH}]_n$ (2a**) in THF at $20 \text{ }^\circ\text{C}$:** A solution of $[\text{NH}_2\text{-BHPH}]_n$ (26 mg, 0.25 mmol) in THF (0.5 mL) was stirred at $20 \text{ }^\circ\text{C}$. After 170 h, the solution was analysed by ^{11}B NMR spectroscopy to reveal partial depolymerisation and redistribution of $[\text{NH}_2\text{-BHPH}]_n$ to yield $\text{H}_2\text{N=BPh}_2$ [δ_{B} 40.6 (br)] (trace amounts), $[\text{HN-BPh}]_3$ [δ_{B} 32.4 (br)] (*ca.* 20 %), $[\text{NH}_2\text{-BHPH}]_n$ [δ_{B} -6.8 (br)] and [δ_{B} -8.0 (br)] (*ca.* 50 %), $\text{NH}_3\cdot\text{BH}_2\text{Ph}$ [δ_{B} -14.0 (t, $^1J_{\text{BH}} = 95 \text{ Hz}$)] (*ca.* 25 %) and $\text{NH}_3\cdot\text{BH}_3$ [δ_{B} -22.8 (q, $^1J_{\text{BH}} = 96 \text{ Hz}$)] (*ca.* 5 %) (Figures S61 and S62). Analysis of the solution by GPC confirmed the presence of high molecular weight polymer ($M_n = 66,000 \text{ g mol}^{-1}$, $M_w = 99,000 \text{ g mol}^{-1}$, PDI = 1.49) (Figure S63).

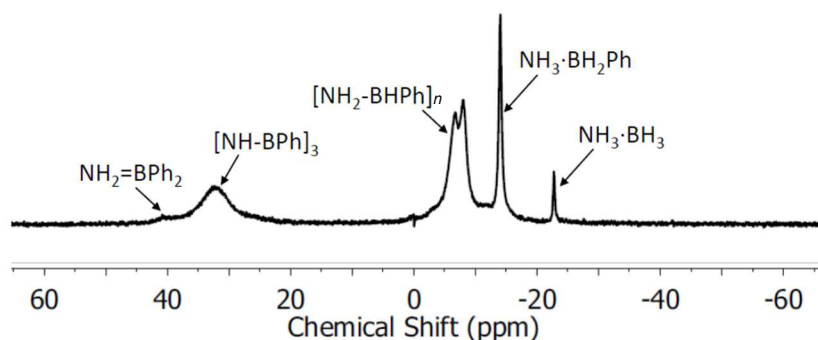


Figure S61. $^{11}\text{B}\{^1\text{H}\}$ NMR spectrum of $[\text{NH}_2\text{-BHPH}]_n$ (**2a**) in THF at $20 \text{ }^\circ\text{C}$ after 170 h.

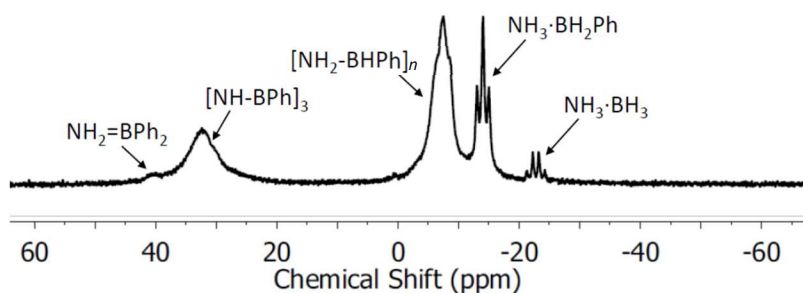


Figure S62. ^{11}B NMR spectrum of $[\text{NH}_2\text{-BHPH}]_n$ (**2a**) in THF at 20 °C after 170 h.

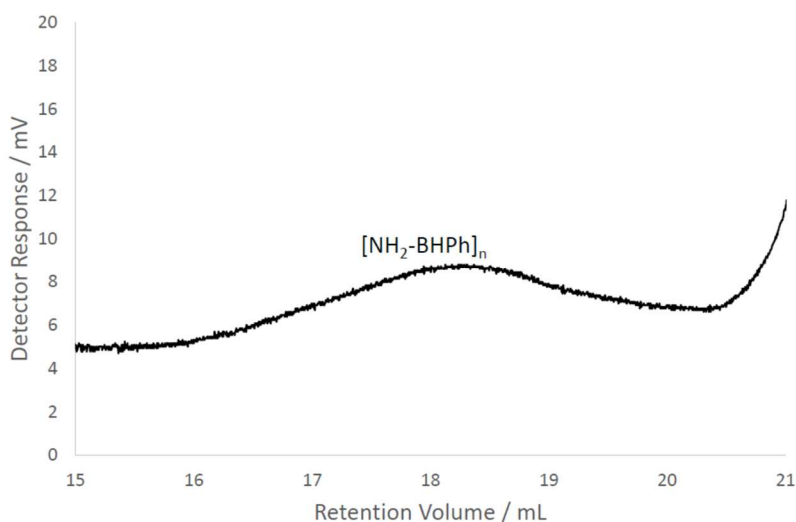


Figure S63. GPC chromatogram (2 mg mL^{-1}) of $[\text{NH}_2\text{-BHPH}]_n$ (**2a**) in THF (0.1 wt% $[n\text{Bu}_4\text{N}]\text{Br}$) at 20 °C after 170 h.

Thermal stability of $[\text{NH}_2\text{-BHPH}]_n$ (2a**) in THF at 70 °C:** An aliquot (0.4 mL) of a solution of $[\text{NH}_2\text{-BHPH}]_n$ (26 mg, 0.25 mmol) in THF (0.5 mL) was transferred to J. Young quartz-glass NMR tube and heated to 70 °C for 170 h. After cooling to 20 °C, the mixture was analysed by ^{11}B NMR spectroscopy indicating partial depolymerisation and redistribution of $[\text{NH}_2\text{-BHPH}]_n$ to yield $\text{H}_2\text{N}=\text{BPh}_2$ [δ_{B} 40.5 (s)] (ca. 5 %), $[\text{HN-BPh}]_3$ [δ_{B} 31.9 (br)] (ca. 70 %), $[\text{NH}_2\text{-BHPH}]_n$ [δ_{B} -6.2 (br)] (ca. 5 %), $\text{NH}_3\cdot\text{BHPH}_2$ [δ_{B} -8.1 (br)] (ca. 15 %), $\text{NH}_3\cdot\text{BH}_2\text{Ph}$ [δ_{B} -14.1 (t, $^1J_{\text{BH}} = 97\text{ Hz}$)] (ca. 5 %), $\text{NH}_3\cdot\text{BH}_3$ [δ_{B} -22.8, (m)] (trace amounts) and $\text{H}_2\text{B}(\mu\text{-H})(\mu\text{-NH}_2)\text{BH}_2$ [δ_{B} -27.6 (br)] (trace amounts) (Figures S64 and S65). Analysis of the solution by GPC revealed that neither high nor low molecular weight polymeric species were present.

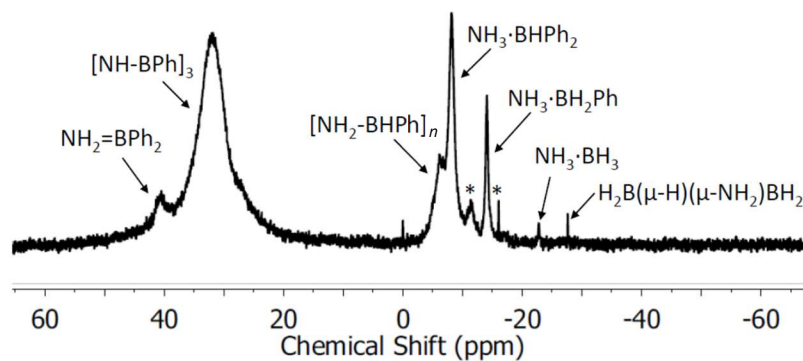


Figure S64. $^{11}\text{B}\{^1\text{H}\}$ NMR spectrum of $[\text{NH}_2\text{-BHPH}]_n$ (**2a**) in THF after heating to 70 °C for 170 h.

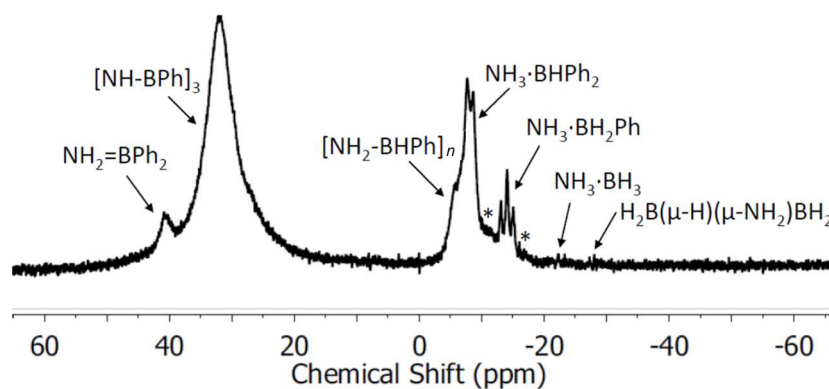


Figure S65. ^{11}B NMR spectrum of $[\text{NH}_2\text{-BHPH}]_n$ (**2a**) in THF after heating to 70 °C for 170 h.

Thermal stability of $[\text{NH}_2\text{-BH}(p\text{-CF}_3\text{C}_6\text{H}_4)]_n$ (2b**) in THF at 20 °C:** A solution of $[\text{NH}_2\text{-BH}(p\text{-CF}_3\text{C}_6\text{H}_4)]_n$ (88 mg, 0.25 mmol) in THF (0.5 mL) was stirred at 20 °C. After 170 h, the solution was analysed by ^{11}B NMR spectroscopy to reveal partial depolymerisation of $[\text{NH}_2\text{-BH}(p\text{-CF}_3\text{C}_6\text{H}_4)]_n$ to yield $[\text{HN-B}(p\text{-CF}_3\text{C}_6\text{H}_4)]_3$ [δ_{B} 32.1 (br)] (*ca.* 35 %), $[\text{NH}_2\text{-BH}(p\text{-CF}_3\text{C}_6\text{H}_4)]_n$ [δ_{B} -7.9 (br)] (*ca.* 45 %), and an unknown species [δ_{B} 12.1 (br)] (*ca.* 20 %) (Figure S66). Analysis of the solution by GPC showed a bimodal distribution containing a high and a low molecular weight fraction (peak at 17.7 mL: $M_{\text{n}} = 72,500 \text{ g mol}^{-1}$, $M_{\text{w}} = 77,500 \text{ g mol}^{-1}$, PDI = 1.07) (peak 18.5 mL: $M_{\text{n}} = 31,500 \text{ g mol}^{-1}$, $M_{\text{w}} = 33,000 \text{ g mol}^{-1}$, PDI = 1.06) (Figure S67).

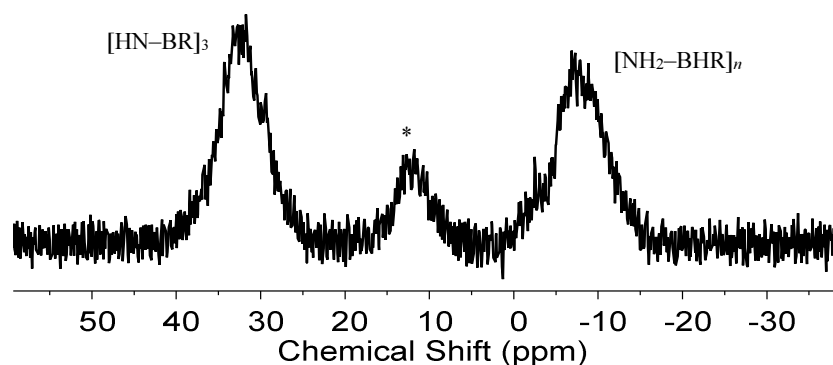


Figure S66. $^{11}\text{B}\{^1\text{H}\}$ NMR spectrum of $[\text{NH}_2\text{-BH}(p\text{-CF}_3\text{C}_6\text{H}_4)]_n$ (**2b**) in THF at 20 °C after 170 h. * Unknown species. R = $p\text{-CF}_3\text{C}_6\text{H}_4$.

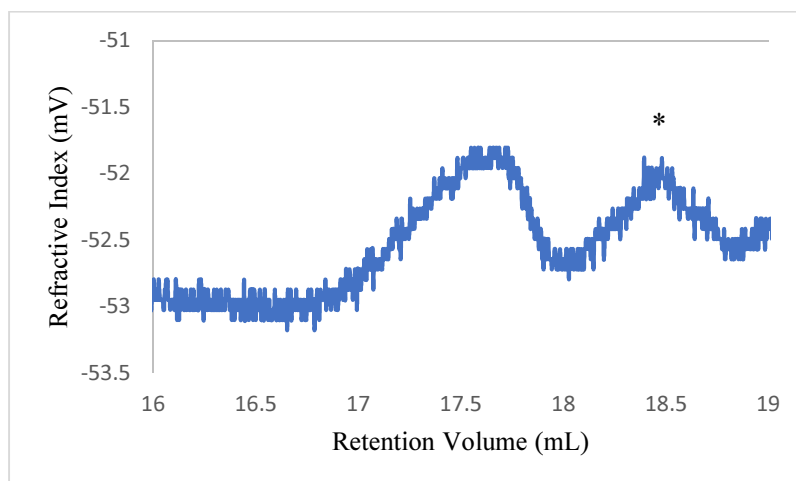


Figure S67. GPC chromatogram (2 mg mL^{-1}) of $[\text{NH}_2\text{-BH}(p\text{-CF}_3\text{C}_6\text{H}_4)]_n$ (**2b**) in THF (0.1 wt% $[\text{nBu}_4\text{N}]\text{Br}$) at 20 °C after 170 h. The asterisk (*) marks an additional trace, which was present in the polymer batch used for the thermal studies.

Thermal stability of $[\text{NH}_2\text{-BH}(p\text{-CF}_3\text{C}_6\text{H}_4)]_n$ (2b**) in THF at 20 °C after three consecutive precipitations:** A solution of $[\text{NH}_2\text{-BH}(p\text{-CF}_3\text{C}_6\text{H}_4)]_n$ (88 mg, 0.25 mmol) in THF (0.5 mL) was stirred at 20 °C. After 170 h, the solution was analysed by ^{11}B NMR spectroscopy to reveal partial depolymerisation of $[\text{NH}_2\text{-BH}(p\text{-CF}_3\text{C}_6\text{H}_4)]_n$ to yield $[\text{HN-B}(p\text{-CF}_3\text{C}_6\text{H}_4)]_3$ [δ_{B} 33.1 (br)] (*ca.* 57 %), $[\text{NH}_2\text{-BH}(p\text{-CF}_3\text{C}_6\text{H}_4)]_n$ [δ_{B} -7.9 (br)] (*ca.* 33 %), and $\text{NH}_3\cdot\text{BH}_2(p\text{-CF}_3\text{C}_6\text{H}_4)$ [δ_{B} -15.0 (br) (t, $^1J_{\text{BH}} = 95\text{ Hz}$)] (*ca.* 10 %) (Figures S68 and S69). Analysis of the solution by GPC showed a bimodal distribution containing a high and a low molecular weight fraction (peak at 17.3 mL: $M_n = 100,000\text{ g mol}^{-1}$, $M_w = 103,800\text{ g mol}^{-1}$, PDI = 1.03) (peak 19.7 mL: $M_n = 7,700\text{ g mol}^{-1}$, $M_w = 9,200\text{ g mol}^{-1}$, PDI = 1.18) (Figure S70).

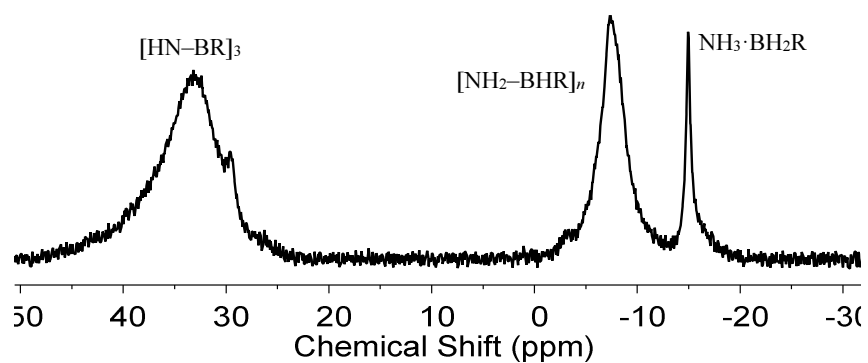


Figure S68. $^{11}\text{B}\{^1\text{H}\}$ NMR spectrum of $[\text{NH}_2\text{-BH}(p\text{-CF}_3\text{C}_6\text{H}_4)]_n$ (**2b**) in THF at 20 °C after 170 h.

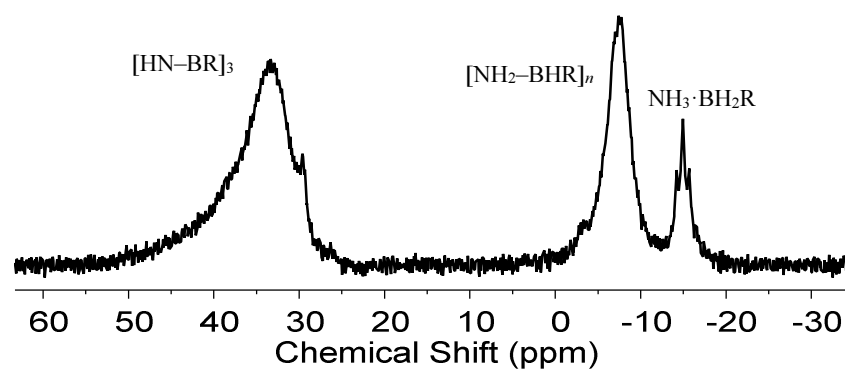


Figure S69. ^{11}B NMR spectrum of $[\text{NH}_2\text{-BH}(p\text{-CF}_3\text{C}_6\text{H}_4)]_n$ (**2b**) in THF at 20 °C after 170 h.

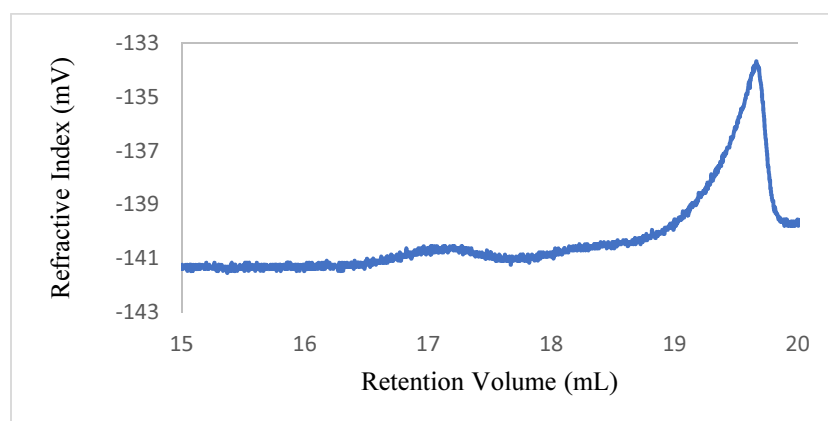


Figure S70. GPC chromatogram (2 mg mL^{-1}) of $[\text{NH}_2\text{-BH}(p\text{-CF}_3\text{C}_6\text{H}_4)]_n$ (**2b**) in THF (0.1 wt% $[\text{nBu}_4\text{N}]\text{Br}$) at 20 °C after 170 h.

Thermal stability of $[\text{NH}_2\text{-BH}(p\text{-CF}_3\text{C}_6\text{H}_4)]_n$ (2b**) in THF at 70 °C:** An aliquot (0.4 mL) of solution of $[\text{NH}_2\text{-BH}(p\text{-CF}_3\text{C}_6\text{H}_4)]_n$ (88 mg, 0.25 mmol) in THF (0.5 mL) was transferred to a J. Young quartz-glass NMR tube and heated to 70 °C for 170 h. After cooling to 20 °C, the mixture was analysed by ^{11}B NMR spectroscopy indicating depolymerisation of $[\text{NH}_2\text{-BH}(p\text{-CF}_3\text{C}_6\text{H}_4)]_n$ to yield $[\text{HN-B}(p\text{-CF}_3\text{C}_6\text{H}_4)]_3$ [δ_{B} 32.7 (br)] (ca. 75 %), $[\text{NH}_2\text{-BH}(p\text{-CF}_3\text{C}_6\text{H}_4)]_x$ [δ_{B} -6.2 and -5.21 (br)] (ca. 15 %) and an unidentified species [δ_{B} 12.3 (br)] (ca. 10 %) (Figures S71 and S72). Analysis of the solution by GPC revealed that neither high nor low molecular weight polymer were present.

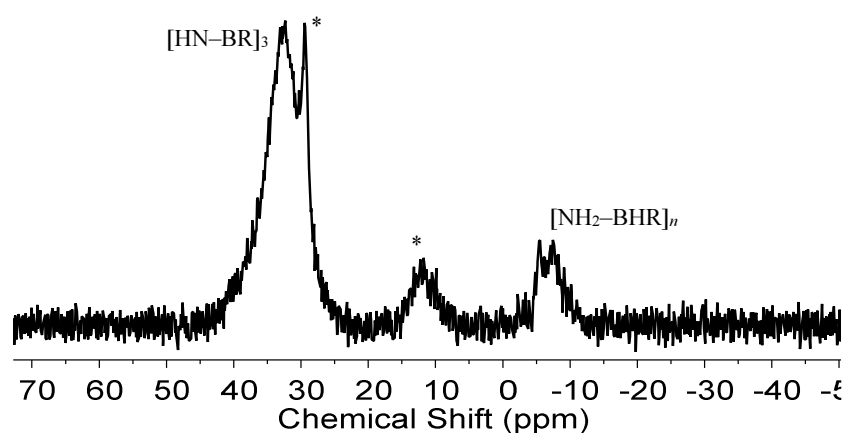


Figure S71. $^{11}\text{B}\{^1\text{H}\}$ NMR spectrum of $[\text{NH}_2\text{-BH}(p\text{-CF}_3\text{C}_6\text{H}_4)]_n$ (**2b**) in THF after heating to 70 °C for 170 h. * Unknown species. R = *p*-CF₃C₆H₄.

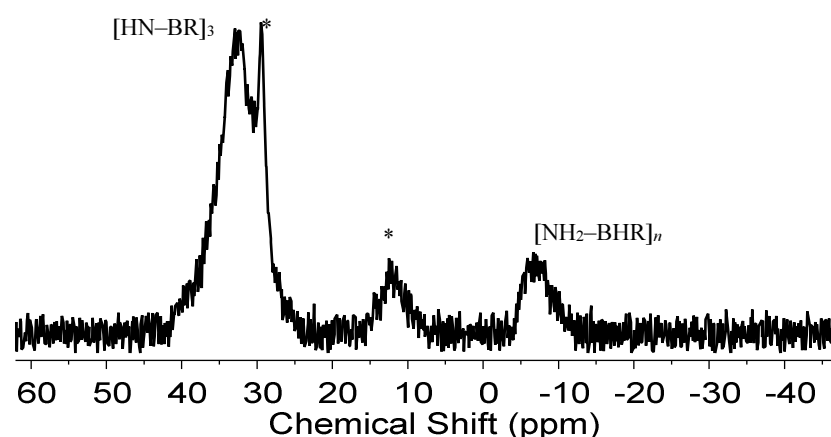


Figure S72. ^{11}B NMR spectrum of $[\text{NH}_2\text{-BH}(p\text{-CF}_3\text{C}_6\text{H}_4)]_n$ (**2b**) in THF after heating to 70 °C for 170 h. * Unknown species. R = *p*-CF₃C₆H₄.

8) References

- S1. Pangborn, A. B.; Giardello, M. A.; Grubbs, R. H.; Rosen, R. K.; Timmers, F. J., Safe and convenient procedure for solvent purification. *Organometallics* **1996**, *15* (5), 1518-1520.
- S2. Gottker-Schnetmann, I.; White, P. S.; Brookhart, M., Synthesis and properties of iridium bis(phosphinite) pincer complexes (p-XPCP)IrH₂, (p-XPCP)Ir(CO), (p-XPCP)Ir(H)(aryl), and {(p-XPCP)Ir}(2){μ-N-2} and their relevance in alkane transfer dehydrogenation. *Organometallics* **2004**, *23* (8), 1766-1776.
- S3. Robertson, A. P. M.; Suter, R.; Chabanne, L.; Whittell, G. R.; Manners, I., Heterogeneous Dehydrocoupling of Amine-Borane Adducts by Skeletal Nickel Catalysts. *Inorg Chem* **2011**, *50* (24), 12680-12691.
- S4. Bruker, *SAINT+ Integration Engine, Data Reduction Software, Bruker Analytical X-ray Instruments Inc., Madison, WI, USA* **2007**.
- S5. Bruker, *SADABS, Bruker AXS area detector scaling and absorption correction, Bruker Analytical X-ray Instruments Inc., Madison, Wisconsin, USA* **2001**.
- S6. Palatinus, L.; Chapuis, G., SUPERFLIP - a computer program for the solution of crystal structures by charge flipping in arbitrary dimensions. *J. Appl. Crystallogr.* **2007**, *40*, 786-790.
- S7. Palatinus, L.; Prathapa, S. J.; van Smaalen, S., EDMA: a computer program for topological analysis of discrete electron densities. *J. Appl. Crystallogr.* **2012**, *45*, 575-580.
- S8. Bourhis, L. J.; Dolomanov, O. V.; Gildea, R. J.; Howard, J. A. K.; Puschmann, H., The anatomy of a comprehensive constrained, restrained refinement program for the modern computing environment-Olex2 dissected. *Acta Crystallographica a-Foundation and Advances* **2015**, *71*, 59-75.
- S9. Sheldrick, G. M., A short history of SHELX. *Acta Crystallogr., Sect. A: Found. Crystallogr.* **2008**, *64*, 112-122.
- S10. Sheldrick, G. M., Crystal structure refinement with SHELXL. *Acta Crystallogr. C* **2015**, *71*, 3-8.
- S11. Dolomanov, O. V.; Bourhis, L. J.; Gildea, R. J.; Howard, J. A. K.; Puschmann, H., OLEX2: a complete structure solution, refinement and analysis program. *J. Appl. Crystallogr.* **2009**, *42*, 339-341.
- S12. Spek, A. L., Single-crystal structure validation with the program PLATON. *J. Appl. Crystallogr.* **2003**, *36*, 7-13.
- S13. Spek, A. L., Structure validation in chemical crystallography. *Acta Crystallographica Section D-Biological Crystallography* **2009**, *65*, 148-155.